

Vertex Nomination, Consistent Estimation, and Adversarial Modification

Joshua Agterberg¹, Youngser Park², Jonathan Larson³, Christopher White³,
Carey E. Priebe^{1,2}, and Vince Lyzinski⁴

¹Department of Applied Mathematics and Statistics, Johns Hopkins University

²Center for Imaging Sciences, Johns Hopkins University

³Microsoft AI and Research, Microsoft

⁴Department of Mathematics and Statistics, University of Massachusetts Amherst University

July 29, 2022

Abstract

Given a pair of graphs G_1 and G_2 and a vertex set of interest in G_1 , the vertex nomination problem seeks to find the corresponding vertices of interest in G_2 (if they exist) and produce a rank list of the vertices in G_2 , with the corresponding vertices of interest in G_2 concentrating, ideally, at the top of the rank list. In this paper we study the effect of an adversarial contamination model on the performance of a spectral graph embedding-based vertex nomination scheme. In both real and simulated examples, we demonstrate that this vertex nomination scheme performs effectively in the uncontaminated setting; adversarial network contamination adversely impacts the performance of our VN scheme; and network regularization successfully mitigates the impact of the contamination. In addition to furthering the theoretic basis of consistency in vertex nomination, the adversarial noise model posited herein is grounded in theoretical developments that allow us to frame the role of an adversary in terms of maximal vertex nomination consistency classes.

1 Introduction and background

Given graphs G_1 and G_2 and vertices of interest $V^* \subset V(G_1)$, the aim of the vertex nomination (VN) problem is to rank the vertices of G_2 into a nomination list with

the corresponding vertices of interest concentrating at the top of the nomination list. In recent years, a host of VN procedures have been introduced (see, for example, [13, 29, 25, 16, 36, 48]) that have proven to be effective information retrieval tools in both synthetic and real data applications. Moreover, recent work establishing a fundamental statistical framework for VN has led to a novel understanding of the limitations of VN efficacy in evolving network environments [26]. Herein, we consider a general statistical model for adversarial contamination in the context of vertex nomination—here the adversary model can both randomly add or remove edges and/or vertices in the network—and we examine the effect of both this contamination and subsequent data regularization (effectively removing outlier nodes) on VN performance. To motivate our mathematical and statistical results further, we first consider an illustrative real data example in Section 1.1 in which we demonstrate the following: A VN scheme that works effectively; network contamination adversely impacting the performance of our VN scheme; and network regularization successfully mitigating the impact of the contamination. Note that we will provide a more thorough background of the relevant literature after the motivating example in Section 1.2.

1.1 Motivating example

Consider the pair of high school friendship networks in [31]: The first, G_1 , has 156 nodes, each representing a student, and has two vertices adjacent if the two students made contact with each other at school in a given time period; the second, G_2 , has 134 vertices, again with each vertex representing a student, and has two vertices adjacent if the two students are friends on Facebook. There are 82 students appearing in both G_1 and G_2 , and we pose the VN problem here as follows: given a student-of-interest in G_1 , can we nominate the corresponding student (if they exist) in G_2 . We note here that the vertex nomination approach outlined below easily adapts to the multiple vertices of interest (v.o.i.) scenario (i.e., given students-of-interest in G_1 , can we nominate the corresponding students, if they exist, in G_2)—and we will provide the necessary details for handling both single and multiple v.o.i. below.

In one idealized data setting, all students would appear in both graphs as this would potentially maximize the signal present in the correspondence of labels across graphs. This bears itself out in the following illustrative VN experiment. Consider the following simple VN scheme, which we denote $\text{VN} \circ \text{GMM} \circ \text{ASE}$: Given vertex (or vertices) of interest v^* in G_1 and seeded vertices $S \subset V_1 \cap V_2$ (seeds here represent vertices whose identity across networks is known a priori), proceed as follows (see Section 4.1 for full detail):

1. Use Adjacency Spectral Embedding (ASE) [43] to separately embed G_1 and G_2 into a common Euclidean space \mathbb{R}^d ;
2. Solve the orthogonal Procrustes problem [39] to find an orthogonal transformation aligning the seeded vertices across graphs; use this transformation to align the embeddings of G_1 and G_2 in \mathbb{R}^d ;
3. Use model-based Gaussian mixture modeling (GMM; e.g., the R package `MClust` [18]) to simultaneously cluster the vertices of the embedded graphs. If $u \in V(G_1)$ and $v \in V(G_2)$ are clustered points in this embedding with respective covariance matrices Σ_u and Σ_v in their components of the GMM, then compute

$$\Delta(u, v) = \max(D_u(u, v), D_v(u, v)),$$

where

$$D_u(u, v) = \sqrt{(u - v)\Sigma_u^{-1}(u - v)^T} \text{ and } D_v(u, v) = \sqrt{(u - v)\Sigma_v^{-1}(u - v)^T}$$

are the respective Mahalanobis distances from u to v .

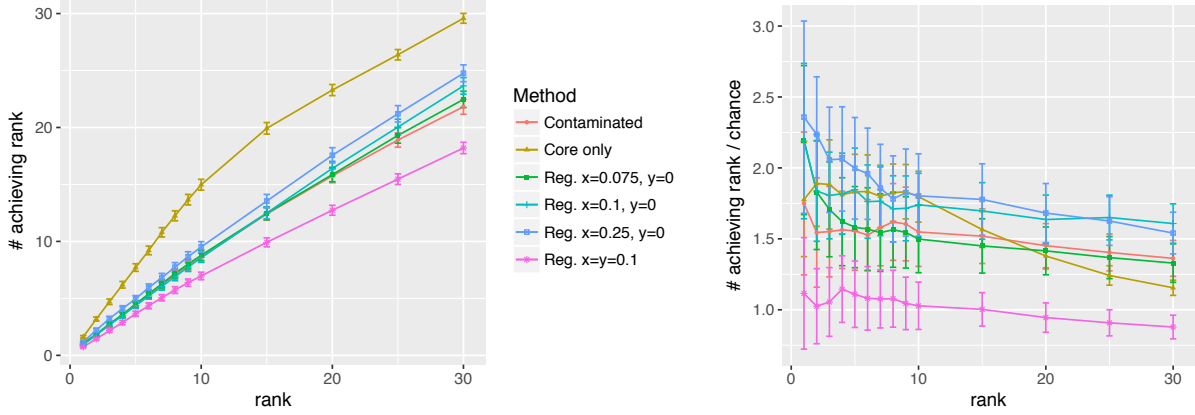
4. In the single v.o.i. setting, rank the candidate v.o.i. in G_2 by increasing value of $\Delta(v^*, u)$ (so that the smallest $\Delta(v^*, u)$ are ranked first). In the multiple v.o.i. setting, we rank the candidate v.o.i. in G_2 by increasing value of $\min_{v \in V^*} \Delta(v, u)$.

We can consider running the above procedure in the idealized data setting where we only consider the induced subgraphs of G_1 and G_2 containing the 82 common vertices across graphs (call these graphs $G_1^{(i)}$ and $G_2^{(i)}$), and we can also consider running the procedure in the setting where the 52 vertices in G_2 without matches across graphs are added to $G_2^{(i)}$ as a form of contamination. These unmatchable vertices can have the effect of obfuscating the correspondence amongst the common vertices across graphs, and thus can diminish VN performance. Indeed, we see this play out in Figure 1.

In Figure 1, we plot the performance of $\text{VN} \circ \text{GMM} \circ \text{ASE}$ averaged over $nMC = 500$ random seed sets of size $s = 10$. In the left figure, the x -axis shows the ranks in the nomination list and the y -axis shows the mean ($\pm 2\text{s.e.}$) number of vertices $v \in G_1^{(i)}$, when viewed as the lone v.o.i., that had their corresponding vertex of interest ranked in the top x by $\text{VN} \circ \text{GMM} \circ \text{ASE}$. The right figure shows the same results normalized by chance performance, where we plot

$$y = \frac{\text{mean \# of v.o.i. with corresp. v.o.i. ranked in top } x \text{ by } \text{VN} \circ \text{GMM} \circ \text{ASE}}{\text{mean \# of v.o.i. with corresp. v.o.i. ranked in top } x \text{ by chance algorithm}}$$

versus x . The gold line represents performance in the idealized networks $G_1^{(i)}$ and $G_2^{(i)}$, and the red line represents performance in the contaminated network pair $(G_1^{(i)}, G_2)$. We see that the contamination detrimentally affects the performance of $\text{VN} \circ \text{GMM} \circ$



a) Mean # achieving rank $\leq x$ versus x

b) Chance normalized mean # achieving rank $\leq x$ versus x

Figure 1: We plot the performance of $\text{VN} \circ \text{GMM} \circ \text{ASE}$ averaged over $nMC = 500$ random seed sets of size $s = 10$. In the left figure, the x -axis shows the ranks in the nomination list and the y -axis shows the mean ($\pm 2\text{s.e.}$) number of vertices $v \in G_1^{(i)}$, when viewed as the v.o.i., that had their corresponding vertex of interest ranked in the top x by $\text{VN} \circ \text{GMM} \circ \text{ASE}$. The right figure shows the same result normalized by chance performance, where we plot ($\pm 2\text{s.e.}$) $y = \frac{\text{mean \# of v.o.i. with corresp. v.o.i. ranked in top } x \text{ by } \text{VN} \circ \text{GMM} \circ \text{ASE}}{\text{mean \# of v.o.i. with corresp. v.o.i. ranked in top } x \text{ by chance algorithm}}$ versus x . The gold line represents performance in the idealized network pair $(G_1^{(i)}, G_2^{(i)})$; the red line for $(G_1^{(i)}, G_2)$; the green line for $(G_1^{(i)}, G_2^{(0.075,0)})$; the teal line for $(G_1^{(i)}, G_2^{(0.1,0)})$; the blue line for $(G_1^{(i)}, G_2^{(0.25,0)})$; and the pink line for $(G_1^{(i)}, G_2^{(0.1,0.1)})$.

Algorithm 1 Regularization via network trimming

Input: Graph G , $x, y \in (0, 1)$, seed set S ;

1. Initialize $V_t = S$
 2. Rank the vertices in $V(G) \setminus S$ by descending degree (ties are broken via averaging over ranks). For each vertex u in $V(G) \setminus S$, denote the rank via $rk(u)$;
- for** $u \in V(G) \setminus S$, **do**
3. If $x < \frac{rk(u)}{|V(G) \setminus S|} \leq y$, add u to V_t ;
- end for**
4. **Output:** $G^{(x,y)} = G[V_t]$, the induced subgraph of G on V_t ;
-

ASE at all levels, as *for all* x , the number of v.o.i. in $G_1^{(i)}$ with their corresponding v.o.i. ranked in the top x in the second graph is larger in $(G_1^{(i)}, G_2^{(i)})$ versus in $(G_1^{(i)}, G_2)$.

How can we mitigate the effect of the contamination in G_2 ? Network regularization is a natural solution, and we here consider as a regularization strategy the network analogue of the classical trimmed mean estimator. To wit, we consider the regularization procedure in Algorithm 1 inspired by the network trimming procedure in [15];

see also the work in [24] for the impact of trimming regularization on random graph concentration.

Remark 1. The parameters x and y appearing in Algorithm 1 are unknown a priori, and to data-adaptively choose x and y , we sweep over possible values and choose the values of x and y that leads to the maximum network modularity in $G_2^{(x,y)}$ when clustering the vertices of $G_2^{(x,y)}$ via $GMM \circ ASE$ clustering; i.e., embed $G_2^{(x,y)}$ using ASE and cluster the embedding using a model-based GMM procedure. Given a clustering C , the modularity is defined as usual via

$$Q(C) = \frac{1}{(2|E|)} \sum_{i,j} \left[A_{i,j} - \frac{d_i d_j}{2|E|} \right] \mathbb{1}\{C_i = C_j\},$$

where $|E|$ = the number of edges in $G_2^{(x,y)}$; $A_{i,j}$ is the i, j -th element of the adjacency matrix A of $G_2^{(x,y)}$; d_i is the degree of vertex i in $G_2^{(x,y)}$; and C_i is the cluster containing vertex i in C .

In the left panel of Figure 2, we plot the modularity of the GMM clustering in the trimmed $G_2^{(x,y)}$ as a function of $x, y \in \{0, 0.05, 0.1, 0.15, 0.2, 0.25\}$. Note that we average the modularity values over $nMC = 500$ seed sets of size $s = 10$ (the same seed sets as used in Figure 1). The color indicates the value of the modularity, with darker red indicating lower values and lighter yellow-to-white indicating larger values. From the figure, we can see that modularity is maximized when $y = 0$ (i.e., no large degree vertices trimmed) and $x \approx 0.05$ – 0.1 . We note that this trimming process can cut core vertices as well as junk vertices, and core vertices cut from G_2 can never be recovered via $VN \circ GMM \circ ASE$. This is demonstrated in the right panel of Figure 2, where the horizontal asymptotes for each trimming value indicates the maximum number of core vertices that are recoverable after regularization.

In Figure 1, we see the effect of regularization play out. Indeed, mean $VN \circ GMM \circ ASE$ performance in the regularized setting increases versus in the contaminated setting for $(x, y) = \{(0.075, 0), (0.1, 0), (0.25, 0)\}$, whereas mean regularized performance decreases for $(x, y) = \{(0.1, 0.1)\}$. From the right figure, we observe that mean performance in the $(x, y) = \{(0.075, 0), (0.1, 0), (0.25, 0)\}$ regularized setting is significantly better than chance, while over-regularizing induces worse than chance performance (the pink line in Figure 1 panel b). While over-regularizing can adversely affect performance, this data-adaptive regularization— while not fully recovering the performance of the idealized setting—nonetheless effectively mitigates the impact of the contamination on our $VN \circ GMM \circ ASE$ algorithm.

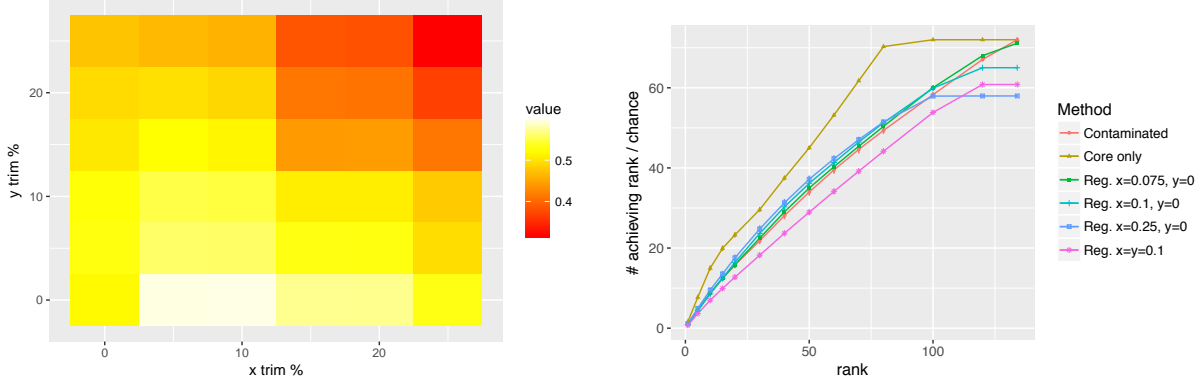


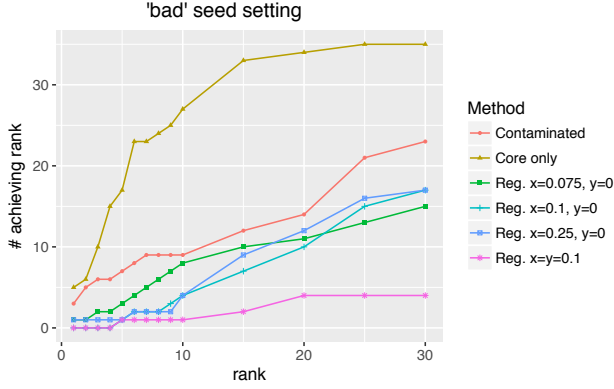
Figure 2: In the left panel, we plot the modularity of the GMM clustering in the trimmed $G_2^{(x,y)}$ as a function of $x, y \in \{0, 0.05, 0.1, 0.15, 0.2, 0.25\}$. Note that we average the modularity values over $nMC = 500$ seed sets of size $s = 10$ (the same seed sets as used in Figure 1). The color indicates the value of the modularity, with darker red indicating lower values and lighter yellow-to-white indicating larger values. In the right panel, we plot the performance of $VN \circ GMM \circ ASE$ averaged over $nMC = 500$ random seed sets of size $s = 10$. In the left figure, the x -axis shows the ranks in the nomination list and the y -axis shows the mean ($\pm 2s.e.$) number of vertices $v \in G_1^{(i)}$, when viewed as the v.o.i., that had their corresponding vertex of interest ranked in the top x by $VN \circ GMM \circ ASE$.

1.1.1 The role of seeds

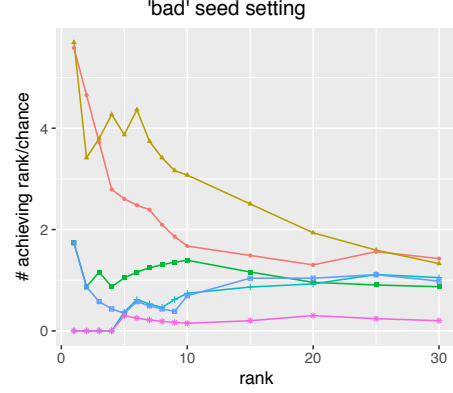
Figure 1 shows performance of $VN \circ GMM \circ ASE$ averaged over 500 randomly chosen seed sets of size 10. While performance, on the whole, increases with proper regularization, the story can vary wildly from seed set to seed set. To demonstrate this, we plot the performance of $VN \circ GMM \circ ASE$ over two particular seed sets (out of the 500 total used in Figure 1) in Figure 3. In the top panels, we plot performance in the setting of “bad” seeds; i.e., those seeds for which the regularization is unable to effectively mitigate the performance loss due to contamination. In the bottom panels, we plot performance in the setting of “good” seeds; i.e., those seeds for which the contamination negatively impacts performance, but subsequent regularization is able to effectively mitigate this performance loss. These two figures (and their respective chance normalizations in the right panels) point to the primacy of seed selection and of understanding what differentiates “good” versus “bad” seeds. While a full exploration of this is beyond the scope of the present text, this is an active area of our work.

1.2 Background

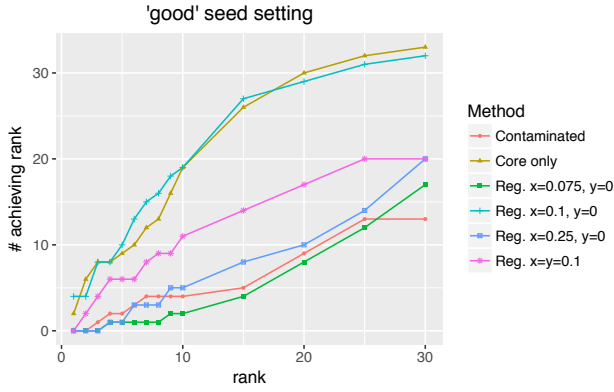
In modern statistics and machine learning, graphs are a common way to take into account the complex relationships between data objects, and graphs have been used



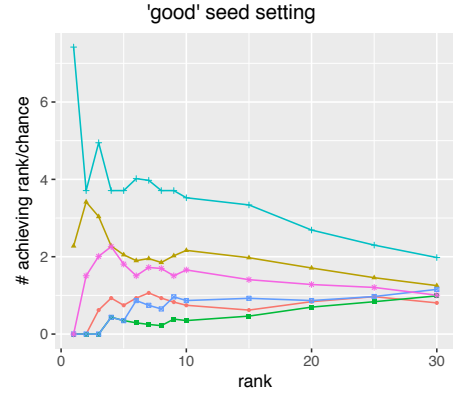
a) # achieving rank $\leq x$ versus x



b) Chance normalized # achieving rank $\leq x$ versus x



c) # achieving rank $\leq x$ versus x



d) Chance normalized # achieving rank $\leq x$ versus x

Figure 3: We plot the performance of $\text{VN} \circ \text{GMM} \circ \text{ASE}$ for two particular seed sets of size $s = 10$. In the top (resp., bottom) panels we plot the performance with “bad” (resp., “good”) seeds. In the left panels, the x -axis shows the ranks in the nomination list and the y -axis shows how many vertices $v \in G_1^{(i)}$, when viewed as the v.o.i., had their corresponding vertex of interest ranked in the top x by $\text{VN} \circ \text{GMM} \circ \text{ASE}$. The right panels shows the same result normalized by chance performance, where we plot $y = \frac{\text{mean \# of v.o.i. with corresp. v.o.i. ranked in top } x \text{ by } \text{VN} \circ \text{GMM} \circ \text{ASE}}{\text{mean \# of v.o.i. with corresp. v.o.i. ranked in top } x \text{ by chance algorithm}}$ vs. x . The gold line represents performance in the idealized network pair $(G_1^{(i)}, G_2^{(i)})$; the red line for $(G_1^{(i)}, G_2)$; the green line for $(G_1^{(i)}, G_2^{(0.075,0)})$; the teal line for $(G_1^{(i)}, G_2^{(0.1,0)})$; the blue line for $(G_1^{(i)}, G_2^{(0.25,0)})$; and the pink line for $(G_1^{(i)}, G_2^{(0.1,0.1)})$.

in applications across the biological (see, for example, [41, 7, 1, 30, 20, 32]) and social sciences (see, for example, [34, 40, 19, 21]). In addition to more traditional statistical inference tasks such as clustering [38, 37, 6, 33], classification [46, 10, 1], and estimation [5, 4, 43], there has been significant work in more network-specific inference tasks such as graph matching [11, 17, 47], and vertex nomination [29, 12, 16].

Loosely speaking, the vertex nomination problem can be stated as follows: given graphs G_1 and G_2 and vertices of interest $V^* \subset V(G_1)$, rank the vertices of G_2 into a nomination list with the corresponding vertices of interest concentrating at the top of the nomination list (see Definition 4 for full detail). While vertex nomination has found applications in a number of different areas, such as social networks in [36] and data associated with human trafficking in [16], there are relatively few results establishing the statistical properties of vertex nomination. In [16], consistency is developed within the stochastic blockmodel random graph framework, where interesting vertices were defined via community membership. In [26], the authors develop the concepts of consistency and Bayes optimality for a very general class of random graph models and a very general definition of what makes the v.o.i. interesting. In this paper, we further develop the ideas in [26], with the aim of developing a theoretical regime in which to ground the notion of adversarial contamination in VN.

There has been significant recent attention towards better understanding the impact of adversarial attacks on machine learning methodologies (see, for example, [23, 8, 35, 14, 50]). Herein, we define an adversarial attack on a machine learning algorithm to be a mechanism that changes the data distribution in order to negatively affect algorithmic performance; see Definition 13. From a practical standpoint, adversarial attacks model the very real problem of having data compromised; if an intelligent agent has access to the data and algorithm, the agent may want to modify the data or the algorithm to give the wrong prediction/inferential conclusion. Although there has been much work on adversarial modeling in machine learning, there has been less theory developed for adversarial attacks from a statistical perspective.

The adversarial framework we consider is similar to the model considered in [8], and it is motivated by the example in the previous section in which the addition of the vertices without correspondences to G_2 negatively impacted VN performance. Suppose that we are interested in performing vertex nomination on a graph pair, but an adversary randomly adds and deletes some edges and/or vertices in the second graph. For example, suppose we are trying to find influencers on Instagram by vertex matching to Facebook. An influencer that has knowledge of our procedure may attempt to make our algorithm fail in its nominations, perhaps by friending and de-friending people on Facebook. Even if our vertex nomination scheme was working well prior to encountering the adversary, it may not be after modification by the adversary. However, if the adversary adds edges/vertices to a graph with some probability and deletes edges/vertices with another probability, it may be possible to partially recover the structure of the original graph by removing vertices with unusual degree behavior [15]. Such a modification is the graph analogue of the “trimmed mean” estimator [42]

from classical statistics.

Empirically, if we assume the adversary is modifying the data randomly, can we still predict whether our VN scheme will perform well on the regularized graph? From a statistical standpoint, what can we say about the statistical consistency of our original vertex nomination rule? Our motivating example suggests that it may be possible to recover performance after regularization, but theory is needed both to explain why that may be the case and to properly frame the problem. Hence, to answer these questions, we further develop the theory in [26] to situate the notion of adversarial contamination within the idea of maximal consistency classes for a given VN rule (Section 2.1). In this framework, the goal of an adversary is to move a model out of a rule’s consistency class, while regularization enlarges the consistency class to (hopefully) thwart the adversary. While we are unable to rigorously establish this for the VN rule, $\text{VN} \circ \text{GMM} \circ \text{ASE}$, considered herein, we demonstrate with real and synthetic data examples that countering such an adversarial attack via network regularization can effectively ameliorate VN performance (Section 4).

Notation: Note that the following notation will be used throughout. For a positive integer k , we will let \mathcal{G}_k denote the set of k -vertex labeled graphs, and we will let $[k] = \{1, 2, 3, \dots, k\}$.

2 Vertex Nomination and Consistency

We will now rigorously define the VN problem and consistency within the VN framework. Combined with the results on consistency classes in Section 2.1, this will allow us to provide a statistical basis for understanding adversarial attacks in VN.

As in our motivating work in [26], we will situate our analysis of the VN problem in the very general framework of nominatable distributions.

Definition 2. For a given $n, m \in \mathbb{Z} > 0$, the set of *Nominatable Distributions of order (n, m)* , denoted $\mathcal{N}_{n,m}$, is the collection of all families of distributions of the following form

$$\mathbf{F}_{\Theta}^{(n,m)} = \{F_{c,\theta}^{(n,m)} \text{ s.t. } 0 \leq c \leq \min(n, m) \in \mathbb{Z}, \theta \in \Theta \subset \mathbb{R}^{d(n,m)}\}$$

where $F_{c,\theta}^{(n,m)}$ is a distribution on $\mathcal{G}_n \times \mathcal{G}_m$ parameterized by $\theta \in \Theta$ satisfying:

1. The vertex sets $V_1 = \{v_1, v_2, \dots, v_n\}$ and $V_2 = \{u_1, u_2, \dots, u_m\}$ satisfy $v_i = u_i$ for $0 < i \leq c$. We refer to $C = \{v_1, v_2, \dots, v_c\} = \{u_1, u_2, \dots, u_c\}$ as the core vertices. These are the vertices that are shared across the two graphs and imbue the model with a natural notion of corresponding vertices.

2. Vertices in $J_1 = V_1 \setminus C$ and $J_2 = V_2 \setminus C$, satisfy $J_1 \cap J_2 = \emptyset$. We refer to J_1 and J_2 as junk vertices. These are the vertices in each graph that have no corresponding vertex in the other graph
3. The induced subgraphs $G_1[J_1]$ and $G_2[J_2]$ are conditionally independent given θ .

The vertices in C are those that have a corresponding paired vertex in each graph; where corresponding can be defined very generally. Corresponding vertices need not correspond to the same person/user/account, rather corresponding vertices are understood as those that share a desired property across graphs. In particular, we will assume that the vertices of interest in G_1 correspond to the vertices of interest in G_2 . Having access to the vertex labels would then render the VN problem trivial. To model the uncertainty often present in data applications, where the vertex labels (or correspondences) are unknown a priori we adopt the notion of *obfuscation functions* from [26].

Definition 3. Let $(G_1, G_2) \sim F_{c,\theta}^{(n,m)} \in \mathcal{N}_{n,m}$, and let W be a set satisfying $W \cap V_i = \emptyset$ for $i = 1, 2$. An obfuscating function $\mathfrak{o} : V_2 \mapsto W$ is a bijection from V_2 to W . We refer to W as an obfuscating set, and we let \mathfrak{D}_W be the set of all such obfuscation functions.

In this framework, a VN scheme is defined as follows.

Definition 4. (VN Scheme) Let $n, m \in \mathbb{Z} > 0$, and for each $g \in \mathcal{G}_m$, $u \in V(g)$, let

$$\mathcal{I}(u; g) = \{w \in V(g) \text{ s.t. } \exists \text{ an automorphism } \sigma \text{ of } g, \text{ s.t. } \sigma(u) = w\}.$$

Let W be an obfuscating set and $\mathfrak{o} \in \mathfrak{D}_W$ be given. For a set A , let \mathcal{T}_A denote the set of all total orderings of the elements of A . A *vertex nomination scheme* is a function $\Phi : \mathcal{G}_n \times \mathfrak{o}(\mathcal{G}_m) \times 2^{V_1} \rightarrow \mathcal{T}_W$ satisfying the following consistency property: If for each $u \in V_2$, we define $\text{rank}_{\Phi(g_1, \mathfrak{o}(g_2), V^*)}(\mathfrak{o}(u))$ to be the position of $\mathfrak{o}(u)$ in the total ordering provided by $\Phi(g_1, \mathfrak{o}(g_2), V^*)$, and we define $\mathfrak{r}_\Phi : \mathcal{G}_n \times \mathcal{G}_m \times \mathfrak{D}_W \times 2^{V_1} \times 2^{V_2} \mapsto 2^{[m]}$ via

$$\mathfrak{r}_\Phi(g_1, g_2, \mathfrak{o}, V^*, S) = \{\text{rank}_{\Phi(g_1, \mathfrak{o}(g_2), V^*)}(\mathfrak{o}(u)) \text{ s.t. } u \in S\},$$

then we require that for any $g_1 \in \mathcal{G}_n$, $g_2 \in \mathcal{G}_m$, $V^* \subset V_1$, obfuscating functions $\mathfrak{o}_1, \mathfrak{o}_2 \in \mathfrak{D}_W$ and any $u \in V(g_2)$,

$$\begin{aligned} \mathfrak{r}_\Phi(g_1, g_2, \mathfrak{o}_1, V^*, \mathcal{I}(u; g_2)) &= \mathfrak{r}_\Phi(g_1, g_2, \mathfrak{o}_2, V^*, \mathcal{I}(u; g_2)) \\ \Leftrightarrow \mathfrak{o}_2 \circ \mathfrak{o}_1^{-1}(\mathcal{I}(\Phi(g_1, \mathfrak{o}_1(g_2), V^*)[k]; \mathfrak{o}_1(g_2))) &= \mathcal{I}(\Phi(g_1, \mathfrak{o}_2(g_2), V^*)[k]; \mathfrak{o}_2(g_2)) \\ &\text{for all } k \in [m], \end{aligned} \tag{1}$$

where $\Phi(g_1, \mathfrak{o}(g_2), V^*)[k]$ denotes the k -th element (i.e., the rank- k vertex) in the ordering $\Phi(g_1, \mathfrak{o}(g_2), V^*)$. We let \mathcal{V}_{nm} denote the set of all such VN schemes.

Remark 5. The consistency criterion, Eq. 1, models the property that a sensibly-defined vertex nomination scheme should view all vertices in a given $\mathcal{I}_g(u)$ as being equally “interesting” in G_2 . These vertices are topologically indistinguishable, and thus are only separated by their labels which have been obfuscated via \mathfrak{o} . Truly obfuscated vertex labels should be independent of the obfuscation function, and the consistency criterion requires that the set of ranks of each set of equivalent vertices (i.e., each $\mathcal{I}_{g_2}(u)$) does not depend on the particular choice of obfuscation function.

A VN scheme is an information retrieval tool for efficiently querying large network data sets. Rather than naively searching G_2 for interesting vertices, an appropriate VN scheme provides a rank list of the vertices in G_2 that, ideally, allows users to identify v.o.i. in G_2 in a time-efficient manner. As such, to measure the performance of a VN scheme, we will adopt a recall-at-k/precision-at-k framework. More precisely, we have

Definition 6. Let $\Phi \in \mathcal{V}_{n,m}$ be a vertex nomination scheme, W an obfuscating set, and $\mathfrak{o} \in \mathfrak{D}_W$. Let (g_1, g_2) be realized from $(G_1, G_2) \sim F_{c\theta}^{(n,m)} \in \mathcal{N}_{n,m}$ with a vertex of interest set $V^* \subset C$. For $k \in [m-1]$, we define the level-k nomination losses via

$$\begin{aligned} \ell_k^{(1)}(\Phi, g_1, g_2, V^*) &:= \frac{\sum_{v \in V^*} \mathbb{1}\{\text{rank}_{\Phi(g_1, \mathfrak{o}(g_2), V^*)}(\mathfrak{o}(v)) \geq k+1\}}{|V^*|} && \text{(recall loss)} \\ &= 1 - \frac{\sum_{v \in V^*} \mathbb{1}\{\text{rank}_{\Phi(g_1, \mathfrak{o}(g_2), V^*)}(\mathfrak{o}(v)) \leq k\}}{|V^*|} \\ \ell_k^{(2)}(\Phi, g_1, g_2, V^*) &:= \frac{\sum_{v \in V^*} \mathbb{1}\{\text{rank}_{\Phi(g_1, \mathfrak{o}(g_2), V^*)}(\mathfrak{o}(v)) \geq k+1\}}{|k|} && \text{(precision loss)} \\ &= \frac{|V^*| - \sum_{v \in V^*} \mathbb{1}\{\text{rank}_{\Phi(g_1, \mathfrak{o}(g_2), V^*)}(\mathfrak{o}(v)) \leq k\}}{|k|}. \end{aligned}$$

The error of a VN scheme is then defined as the expected loss. To wit, we have

Definition 7. Let $\Phi \in \mathcal{V}_{n,m}$ be a vertex nomination scheme, W an obfuscating set, and $\mathfrak{o} \in \mathfrak{D}_W$. The level- k error of Φ for $V^* \subset C$ and $F_{c,\theta}^{(n,m)} \in \mathcal{N}$ is defined as

$$\begin{aligned} L_k^{(1)}(\Phi, V^*) &:= \mathbb{E}_{(G_1, G_2) \sim F_{c,\theta}^{(n,m)}}[\ell_k^{(1)}(\Phi, G_1, G_2, V^*)] && \text{(recall error)} \\ &= \frac{1}{|V^*|} \sum_{v \in V^*} \mathbb{P}_{(G_1, G_2) \sim F_{c,\theta}^{(n,m)}}\left(\text{rank}_{\Phi(G_1, \mathfrak{o}(G_2), V^*)}(\mathfrak{o}(v)) \geq k+1\right) \\ L_k^{(2)}(\Phi, V^*) &:= \mathbb{E}_{(G_1, G_2) \sim F_{c,\theta}^{(n,m)}}[\ell_k^{(2)}(\Phi, G_1, G_2, V^*)] && \text{(precision error)} \\ &= \frac{1}{|k|} \sum_{v \in V^*} \mathbb{P}_{(G_1, G_2) \sim F_{c,\theta}^{(n,m)}}\left(\text{rank}_{\Phi(G_1, \mathfrak{o}(G_2), V^*)}(\mathfrak{o}(v)) \geq k+1\right) \end{aligned}$$

The *level-k Bayes optimal scheme* is defined as any element

$$\Phi_{k, V^*}^* \in \text{argmin}_{\phi \in \mathcal{V}_{nm}} L_k^{(1)}(\Phi, V^*) = \text{argmin}_{\phi \in \mathcal{V}_{nm}} L_k^{(2)}(\Phi, V^*),$$

with corresponding errors $L_k^{*,(1)}$ and $L_k^{*,(2)}$.

In the absence of symmetries amongst the vertices in V^* (i.e., $\mathcal{I}(v, G_2) = \{v\}$ for all $v \in V^*$), the derivation of the Bayes optimal scheme in the present $|V^*| > 1$ setting mimics that of the $|V^*| = 1$ setting presented in [26]. See Appendix A for full detail. Bayes optimal schemes when symmetries exist for the v.o.i., i.e. $|\mathcal{I}(v; g_2)| > 1$, offer additional complications and, in the case when $|V^*| = 1$ done in [26], little additional insight. Precisely defining the Bayes optimal scheme in the case of symmetries when $|V^*| > 1$ is notationally and technically nontrivial, and is the subject of current research. Consistency in the VN framework is then defined as follows.

Definition 8. Let $\mathbf{F} = \left(F_{c_n, \theta_n}^{(n, m_n)}\right)_{n=n_0}^\infty$ be a sequence of distributions in \mathcal{N} . We say that \mathbf{F} has *nested cores* if there exists an n_1 such that for all $n_1 \leq n < n'$, if $(G_1, G_2) \sim F_{c_n, \theta_n}^{(n, m_n)}$ and $(G'_1, G'_2) \sim F_{c_{n'}, \theta_{n'}}^{(n', m_{n'})}$, we have, letting C and C' be the core vertices associated with $F_{c_n, \theta_n}^{(n, m_n)}$ and $F_{c_{n'}, \theta_{n'}}^{(n', m_{n'})}$ respectively, and denoting the junk vertices J_1, J'_1, J_2, J'_2 analogously,

- i. $V(G_1) = C \cup J_1 \subset V(G'_1) = C' \cup J'_1$;
- ii. $V(G_2) = C \cup J_2 \subset V(G'_2) = C' \cup J'_2$;
- iii. $C \subset C'$.

Definition 9. Let $\mathbf{F} = (F_{c_n, \theta_n}^{(n, m_n)})_{n=n_0}^\infty$ be a sequence of nominatable distributions in \mathcal{N} with nested cores satisfying $\lim_{n \rightarrow \infty} m_n = \infty$. For a given non-decreasing sequence (k_n) , we say that a VN rule $\Phi = (\Phi_{n, m_n})_{n=n_0}^\infty$ is

- i. level- (k_n) recall consistent for nested $V_n^* \in C_n$ with respect to \mathbf{F} if

$$\lim_{n \rightarrow \infty} L_{k_n}^{(1)}(\Phi_{n, m_n}, V_n^*) - L_{k_n}^{*,(1)}(V_n^*) = 0,$$

for any sequence of obfuscating functions of V_2 with $|V_2| = m_n$.

- ii. level- (k_n) precision consistent for nested $V_n^* \in C_n$ with respect to \mathbf{F} if

$$\lim_{n \rightarrow \infty} L_{k_n}^{(2)}(\Phi_{n, m_n}, V_n^*) - L_{k_n}^{*,(2)}(V_n^*) = 0,$$

for any sequence of obfuscating functions of V_2 with $|V_2| = m_n$.

We say that a VN rule Φ is *universally level- (k_n) $\left(\frac{\text{precision}}{\text{recall}}\right)$ consistent* if it is level- (k_n) $\left(\frac{\text{precision}}{\text{recall}}\right)$ consistent for all nested-core nominatable sequences \mathbf{F} . Corollary 19 from [26] proves that universally consistent VN schemes do not exist for any nondecreasing integral sequences (k_n) satisfying $k_n = o(m_n)$ and any (V_n^*) satisfying $|V_n^*| = \Theta(1)$. Beyond the ramifications for practically implementing VN in streaming or evolving network environments considered in [26], this lack of universal consistency is also the

motivating result for our statistical approach to adversarial contamination in VN. Indeed, a simple consequence of the lack of universal consistency is that for any VN rule there are nominatable sequences for which the rule is not consistent. An adversary could then be understood as a probabilistic mechanism designed to transform nominatable sequences for which the rule is consistent into nominatable sequences for which the rule is not consistent.

To develop this reasoning further, we next develop the notion of (maximal) consistency classes in the VN framework.

2.1 VN Consistency Classes

We next explore the concept of consistency classes in VN, with an eye towards the development of a statistical adversarial contamination framework for VN. First, let $\mathfrak{N}_{\mathbf{V}^*}$ be the collection of all nested-core nominatable sequences with nested v.o.i. $\mathbf{V}^* = (V_n^* \subset C_n)$. For a given VN rule Φ , v.o.i. sequence \mathbf{V}^* satisfying $|V_n^*| = \Theta(1)$, and nondecreasing sequence (k_n) (satisfying the growth conditions of Lemma 11), the level- (k_n) $\binom{\text{precision}}{\text{recall}}$ consistency class of Φ is defined to be

$$\mathfrak{C}_{\Phi}^{(k_n)} = \left\{ \mathbf{F} \in \mathfrak{N}_{\mathbf{V}^*} \text{ s.t. } \Phi \text{ is level-}(k_n) \binom{\text{precision}}{\text{recall}} \text{ consistent for } \mathbf{F} \right\}.$$

The lack of universal consistency ensures that $\mathfrak{C}_{\Phi}^{(k_n)} \neq \mathfrak{N}_{\mathbf{V}^*}$ for any rule Φ .

It is natural to ask if there are a finite number of VN rules $\{\Phi_i\}$ such that $\cup_i \mathfrak{C}_{\Phi_i}^{(k_n)} = \mathfrak{N}_{\mathbf{V}^*}$. An affirmative answer would allow for ensemble methods to practically overcome the lack of universally consistent rules, and hence practically overcome any adversarial attack in the VN framework. We will see in Section 2.1.1 that the answer is, as expected, no, and any partition of $\mathfrak{N}_{\mathbf{V}^*}$ into maximal consistency classes necessarily contains infinite parts; see Lemma 11. As a consequence, ensemble methods cannot recover universal consistency in VN. The insights developed in Section 2.1.1 further motivate the development of adversarial contamination regimes for a given rule Φ . The idea behind adversarial contamination is simple in this framework: the adversary contaminates elements $\mathbf{F} \in \mathfrak{C}_{\Phi}^{(\mathbf{k}_n)}$ transforming them into $\mathbf{F}' \in \mathfrak{N}_{\mathbf{V}^*} \setminus \mathfrak{C}_{\Phi}^{(\mathbf{k}_n)}$.

2.1.1 Counting Consistency Classes

How can a practitioner mitigate the impact of a lack of universal consistency? One idea would be to consider ensemble methods, as the practical implications of the lack of universal consistency can be mitigated if universally consistent ensemble schemes exist. In this section, we will formalize the notion of maximal VN consistency classes and

prove that infinitely many maximal consistency classes exist. We begin with defining the notion of maximal consistency classes in the VN-framework.

Definition 10. As above, let $\mathfrak{N}_{\mathbf{V}^*}$ be the collection of all nested-core nominatable sequences with nested v.o.i. $\mathbf{V}^* = (V_n^* \subset C_n)$. For a nondecreasing integer sequence (k_n) , we say that $\mathfrak{C} \in \mathfrak{N}_{\mathbf{V}^*}$ is a maximal level- (k_n) $\binom{\text{precision}}{\text{recall}}$ consistency class for \mathbf{V}^* if the following two conditions hold.

- i. There exists a VN rule Φ that is jointly level- (k_n) $\binom{\text{precision}}{\text{recall}}$ consistent for \mathbf{V}^* for each $\mathbf{F} \in \mathfrak{C}$;
- ii. If $\mathbf{F}' \notin \mathfrak{C}$, then there does not exist a VN rule Φ that is jointly level- (k_n) $\binom{\text{precision}}{\text{recall}}$ consistent for \mathbf{V}^* for each $\mathbf{F} \in \mathfrak{C} \cup \{\mathbf{F}'\}$.

A natural question to ask is whether it is possible to partition $\mathfrak{N}_{\mathbf{V}^*}$ into a finite number of maximal level- (k_n) consistency classes for a particular sequence $(k_n)_{n=1}^\infty$? Our next result—Lemma 11—shows that for any integer sequence (k_n) satisfying a modest growth condition, any partition of \mathfrak{N} into maximal level- (k_n) consistency classes must include at least countably infinite parts, thus erasing the hope that ensemble methods can recover universal consistency and practically mitigate the effect of any VN adversarial attack.

Lemma 11. *Let (k_n) be a sequence of nondecreasing integers satisfying $k_n = o(n)$, and let \mathbf{V}^* be a nested sequence of vertices of interest satisfying $|V_n^*| = \Theta(1)$.*

- i. *Let $\mathfrak{N}_{\mathbf{V}^*} = \cup_{\alpha \in \mathcal{A}} \mathfrak{C}_\alpha$ be a partition of $\mathfrak{N}_{\mathbf{V}^*}$ into maximal level- (k_n) recall consistency classes, then $|\mathcal{A}| = \infty$.*
- ii. *Let $\mathfrak{N}_{\mathbf{V}^*} = \cup_{\alpha \in \mathcal{A}} \mathfrak{C}_\alpha$ be a partition of $\mathfrak{N}_{\mathbf{V}^*}$ into maximal level- (k_n) precision consistency classes. If $k_n = \Theta(1)$, then $|\mathcal{A}| = \infty$.*

The proof of this lemma can be found in Appendix B

2.1.2 Verification functions

In the presence of an adversarial attack, is it possible to, without additional supervision, verify if a given VN scheme is working on a given $F_{c,\theta}^{(n,m)} \in \mathcal{N}_{n,m}$? In other words, given a nondecreasing integer sequence (k_n) , $(g_1, g_2) \in \mathcal{G}_n \times \mathcal{G}_m$, and v.o.i. V_n^* , can we consistently estimate the *verification function*

$$h_{\Phi_n}(g_1, \mathfrak{o}(g_2), V_n^*) = h_{\Phi_n, v, \mathfrak{o}_n, k_n}(g_1, \mathfrak{o}_n(g_2)) = \sum_{v \in V_n^*} \mathbb{1} \{ \text{rank}_{\Phi_n(g_1, \mathfrak{o}_n(g_2), V_n^*)}(\mathfrak{o}(v)) \leq k_n \}?$$

Note that the scaling by $|V_n^*|$ in the recall setting and by k_n in the precision setting do not affect consistent estimation of h given $|V_n^*| = \Theta(1)$ and in the precision setting $k_n = \Theta(1)$. As such, the scaling is omitted.

The internal consistency criterion, Eq. 1 guarantees that

$$h_{\Phi_n}(g_1, \mathfrak{o}_n(g_2), V_n^*) = h_{\Phi_n}(g_1, \tilde{\mathfrak{o}}_n(g_2), V_n^*) \quad (2)$$

for all obfuscation functions $\mathfrak{o}_n, \tilde{\mathfrak{o}}_n \in \mathfrak{D}_n$. Indeed, the v.o.i.'s in g_2 are identical (though obfuscated differently) in $\mathfrak{o}_n(g_2)$ and $\tilde{\mathfrak{o}}_n(g_2)$. If we consider an alternate $(g'_1, g'_2) \sim F'_n \subset \mathbf{F}'$, it could be the case that $g_1 = g'_1$ and $g_2 \approx g'_2$, while $h_{\Phi_n}(g_1, \mathfrak{o}_n(g_2), V_n^*) \neq h_{\Phi_n}(g_1, \tilde{\mathfrak{o}}_n(g_2), V_n^*)$ for any $\mathfrak{o}_n \in \mathfrak{D}_n$; indeed, consider letting the v.o.i.'s' in g'_2 be different from those in g_2 (i.e., the behavior of the v.o.i. in F'_n is different from the behavior of the v.o.i. in F_n).

Consider the problem of estimating h_{Φ_n} via \hat{h}_{Φ_n} . If the estimator is label-agnostic (i.e., there is no information in the obfuscated labeling of $\mathfrak{o}(g_2)$), then it is sensible to require that for all $g_2 \approx g'_2$, we have that

$$\hat{h}_{\Phi_n}(g_1, \mathfrak{o}_n(g_2), V_n^*) = \hat{h}_{\Phi_n}(g_1, \tilde{\mathfrak{o}}_n(g_2), V_n^*) \quad (3)$$

Contrasting this to Eq. (2), we see that (\hat{h}_{Φ_n}) cannot universally consistently estimate (h_{Φ_n}) , as the sequence of estimators cannot account for the potentially different behaviors of the v.o.i.'s under the umbrella of nominatable distributions. To wit, we have the following lemma.

Lemma 12. *With notation as above, let $(\hat{h}_{\Phi_n})_n$ be any sequence of label-agnostic (i.e., satisfying Eq. 3) estimators of $(h_{\Phi_n})_n$. There exists sequences of nested-core nominatable distributions $\mathbf{F} = (F_n)$ and $\mathbf{F}' = (F'_n)$ such that for n sufficiently large, if $(G_1, G_2) \sim F_n$, and $(G'_1, G'_2) \sim F'_n$, then*

$$d_{TV}(\mathcal{L}(h_{\Phi_n}(G_1, \mathfrak{o}(G_2), V_n^*)), \mathcal{L}(h_{\Phi_n}(G'_1, \mathfrak{o}(G'_2), V_n^*))) > 0,$$

while $\mathcal{L}(\hat{h}_{\Phi_n}(G_1, \mathfrak{o}(G_2), V_n^*)) = \mathcal{L}(\hat{h}_{\Phi_n}(G'_1, \mathfrak{o}(G'_2), V_n^*))$ (where d_{TV} is the total variation distance).

As a result of the above discussion and Lemma, we are unable to verify, without additional supervision, if an adversary has moved the distribution out of a given VN rule's consistency class. This points to the primacy of additional supervision, which in the VN framework often comes in the form of a user-in-the-loop. Indeed, we are currently exploring the role/impact a use-in-the-loop in VN—where the user can evaluate the interestingness of the vertices in the top k of the nomination list for a cost c_k . This supervision can also be thought of as a form of regularization, designed to increase the consistency class of a given VN rule.

3 Adversarial Vertex Nomination

In order to actively model adversarial attacks in the VN-framework, we formalize the notion of an *edge adversary*.

Definition 13. Let F be a distribution on graphs in \mathcal{G}_m , and let U be a random variable independent of $G \sim F$. We say $\mathcal{A} = \{f_{\mathcal{A}}, V_{\mathcal{A}}, U, \theta\}$ is an *adversary* parameterized by $\theta \in \Theta$ if

1. $f_{\mathcal{A}} : \mathcal{G}_m \times \mathbb{R} \times \Theta \mapsto \mathcal{G}_m$ is a measurable function such that $V(f_{\mathcal{A}}(G, U, \theta)) = V(G)$, so that $f_{\mathcal{A}}(G, U, \theta)$ is a \mathcal{G}_m -valued random variable.
2. $V_{\mathcal{A}} : \mathcal{G}_m \times \mathbb{R} \times \Theta \mapsto 2^{[m]}$ is a measurable function that satisfies $V_{\mathcal{A}}(G, U, \theta) \subset V(G)$, so that $V_{\mathcal{A}}(G, U, \theta)$ is a (potentially) random subset of $V(G)$.
3. If $K = \left\{ v, w \in V(G) \text{ s.t. } (v, w) \in E(f_{\mathcal{A}}(G, U, \theta)) \Delta E(G) \right\}$, (where Δ represents the symmetric difference) then $K \subset V_{\mathcal{A}}(G, U, \theta)$. Succinctly put, if an edge is added or removed from $E(G)$, then the vertices adjacent to that edge must be in $V_{\mathcal{A}}(G, U, \theta)$.

In the above, U represents an independent source of randomness utilized in the adversarial attack.

Note that $f_{\mathcal{A}}$ is simply a function that adds/deletes edges from a network potentially randomly, and these edges must be incident to the vertices of $V_{\mathcal{A}}$. To that end, we will refer to $V_{\mathcal{A}}$ as the vertices *contaminated* by \mathcal{A} .

If we are given a sequence of nominatable distributions $\mathbf{F} = (F_n)_{n=n_0}^{\infty}$, where F_n is a distribution on $\mathcal{G}_n \times \mathcal{G}_m$, then we will let $f_{\mathcal{A}_n}(F_n)$ denote a sequence of graphs realized from F_n , with the second graph G_2 contaminated by $f_{\mathcal{A}_n}$; we call a sequence $(f_{\mathcal{A}_n})_{n=n_0}^{\infty}$ an adversary rule. In the language of VN consistency classes, we posit that an adversary rule aims to contaminate a VN rule Φ via

$$\mathbf{F} = (F_n)_{n=n_0}^{\infty} \in \mathfrak{C}_{\Phi}^{(k_n)} \implies (f_{\mathcal{A}_n}(F_n))_{n=n_0}^{\infty} \in \mathfrak{N}_{\mathbf{V}^*} \setminus \mathfrak{C}_{\Phi}^{(k_n)}.$$

Remark 14. Let $G_2 = (V_2, E_2)$ and $G'_2 = (V'_2, E'_2)$. Consider an edge adversary $f_{\mathcal{A}}$ acting on G'_2 . By considering $V_2 = V(G'_2) \setminus V_{\mathcal{A}}$, we can also consider this adversary as a *vertex adversary* that randomly adds vertices to G_2 . Vertex addition and deletion can be simultaneously modeled by first considering a mechanism for randomly deleting vertices from $G_2 = (V_2, E_2)$ before using the above approach to add adversarial vertices to the network.

Remark 15. In [50], the authors consider *direct attacks* and *influencer attacks* in which, given a vertex of interest v^* , either $v^* \in V_{\mathcal{A}}$ or $v^* \notin V_{\mathcal{A}}$ respectively. However, note

that in [50], the objective is vertex classification, whereas we are not directly classifying vertices. Rather, we are interested in ranking vertices in G_2 by interestingness given limited training data in G_1 . We will typically assume that $v^* \notin V_{\mathcal{A}}$ (i.e. the adversary does not control the vertex of interest), so that we are examining *influencer attacks*.

3.1 A Simple VN Adversarial Contamination Model

Now that we have developed the requisite theory for framing the idea of adversarial contamination in the VN-setting, we will consider a simple model for adversarial contamination in the stochastic blockmodel (SBM) of [22].

Definition 16. We say that an n -vertex random graph G is an instantiation of a stochastic blockmodel with parameters (n, K, B, b) (written $A \sim \text{SBM}(n, K, B, \pi)$) if

- i. The block membership vector $\pi \in \mathbb{R}^K$ satisfies $\pi_i \geq 0$ for all $i \in [K]$, and $\sum_i \pi(i) = 1$;
- ii. The vertex set $V = V(G)$ is the disjoint union of K blocks $V = B_1 \sqcup B_2 \sqcup \dots \sqcup B_K$, where each vertex $v \in V$ is independently assigned to a block according to a Multinomial($1, \pi$) distribution. If vertex v is assigned to block $i \in [K]$, then the block membership function $b : V \mapsto [K]$ satisfies $b(v) = i$;
- iii. The block probability matrix $B \in [0, 1]^{K \times K}$ is such that, for each pair of vertices $\{u, v\} \in \binom{V}{2}$, $\mathbb{1}_{u \sim_G v} \sim \text{Bernoulli}(B_{b(u), b(v)})$, and the collection of indicator random variables $\{\mathbb{1}_{u \sim_G v}\}_{\{u, v\} \in \binom{V}{2}}$ is mutually independent (here $\{u \sim_G v\} \Leftrightarrow \{\{u, v\} \in E\}$).

In addition, we will say that a pair of graphs (G_1, G_2) is an instantiation of a ρ -correlated $\text{SBM}(n, K, B, b)$ (written $(G_1, G_2) \sim \text{SBM}(\rho, n, K, B, \pi)$) if marginally $G_1 \sim \text{SBM}(n, K, B, b)$ and $G_2 \sim \text{SBM}(n, K, B, b)$, and the collection of indicator random variables

$$\left\{ \left\{ \mathbb{1}_{u \sim_{G_1} v} \right\}_{\{u, v\} \in \binom{V}{2}} \cup \left\{ \mathbb{1}_{u \sim_{G_2} v} \right\}_{\{u, v\} \in \binom{V}{2}} \right\}$$

is mutually independent except that for each $\{u, v\} \in \binom{V}{2}$, $\text{Corr}(\mathbb{1}_{u \sim_{G_1} v}, \mathbb{1}_{u \sim_{G_2} v}) = \rho$.

Consider G as an n -vertex stochastic blockmodel, with two blocks, B_1 and B_2 , and with $\pi = (1/2, 1/2)$. The block-probability matrix B is given by

$$B = \begin{pmatrix} p & r \\ r & q \end{pmatrix}, \tag{4}$$

with $p \geq q \geq r > 0$. Given $G = g$, we define the following VN adversarial contamination procedure $\mathcal{A} = (f_{\mathcal{A}}, V_{\mathcal{A}}, U, \theta)$ acting on g as follows:

1. $\theta = (c_+, c_-, \pi_+, \pi_-, s_+, s_-)$ is a vector of parameters where $c_+, c_- \in \mathbb{Z}$ satisfy $c_+ + c_- \leq n$, $\pi_+, \pi_- \in (0, 1)$, and $s_+, s_- \in [0, 1]$;
2. U is a uniformly distributed random variable independent of G ;
3. $f_{\mathcal{A}}(g, U, \theta) \in \mathcal{G}_n$ is defined as follows:
 - i. Initialize $g_c = g$
 - ii. Independently select vertices from $V = [n]$ with probability π_+ (call them W_+). Then, independently select vertices $V \setminus W_+$ with probability π_- (call them W_-).
 - iii. For each vertex pair $\{v, u\} \in W_+ \times (V \setminus W_-)$,
 - i. If $\{v, u\} \in E(g_c)$, nothing happens.
 - ii. If $\{v, u\} \notin E(g_c)$, an edge is independently added connecting $\{v, u\}$ in g_c with probability s_+ .
 - iv. For each vertex pair $\{v, u\} \in W_- \times (V \setminus W_+)$,
 - i. If $\{v, u\} \notin E(g_c)$, nothing happens.
 - ii. If $\{v, u\} \in E(g_c)$, the edge is independently deleted from g_c with probability s_- .
 - v. Set $f_{\mathcal{A}}(g, U, \theta) = g_c \in \mathcal{G}_n$.

The auxiliary randomness U in \mathcal{A} is utilized to make the random vertex selections in ii., the random edge additions in iii., and the random edge deletions in iv.

Notice that this adversarial model gives rise to a new stochastic blockmodel with the edge-probability matrix \tilde{B} given by

$$\tilde{B} = \begin{matrix} & \tilde{B}_1 & \tilde{B}_1^+ & \tilde{B}_1^- & \tilde{B}_2 & \tilde{B}_2^+ & \tilde{B}_2^- \\ \begin{matrix} \tilde{B}_1 \\ \tilde{B}_1^+ \\ \tilde{B}_1^- \\ \tilde{B}_2 \\ \tilde{B}_2^+ \\ \tilde{B}_2^- \end{matrix} & \begin{pmatrix} \mathbf{p} & x_1 & x_2 & \mathbf{r} & x_3 & x_4 \\ x_1 & x_1 & p & x_3 & x_5 & r \\ x_2 & p & x_2 & x_4 & r & x_6 \\ \mathbf{r} & x_3 & x_4 & \mathbf{q} & x_7 & x_8 \\ x_3 & x_5 & r & x_7 & x_7 & q \\ x_4 & r & x_6 & x_8 & q & x_8 \end{pmatrix} \end{matrix}$$

where

$$\begin{aligned} x_1 &= p + s_+(1-p), & x_2 &= p(1-s_-), & x_3 &= r + s_+(1-r), \\ x_4 &= (1-s_-)r, & x_5 &= r + (2s_+ - s_+)^2(1-r), & x_6 &= r(1-s_-)^2 \\ x_7 &= q + s_+(1-q), & x_8 &= q(1-s_-), \end{aligned}$$

and where \tilde{B}_1^+ are the vertices in $W_+ \cap B_1$; \tilde{B}_1^- are the vertices in $B_1 \cap W_-$; and \tilde{B}_1 are the vertices in $B_1 \setminus (\tilde{B}_1^+ \cup \tilde{B}_1^-)$; with \tilde{B}_2 defined analogously. We note here that this adversarial contamination model is similar to the contamination model considered in [8].

Note also that the original block structure is preserved amongst vertices in $\tilde{B}_1 \cup \tilde{B}_2$, and we can view this contamination model as adding vertices randomly to $G[\tilde{B}_1 \cup \tilde{B}_2]$, i.e., the induced subgraph on $\tilde{B}_1 \cup \tilde{B}_2$. When $(G_1, G_2) \sim \text{SBM}(\rho, n, K, B, \pi)$ and this adversarial procedure is applied to G_2 , we will denote

$$G_1^{(i)} = G_1[\tilde{B}_1 \cup \tilde{B}_2] \quad (5)$$

$$G_2^{(i)} = G_2[\tilde{B}_1 \cup \tilde{B}_2] \quad (6)$$

Remark 17. Let \mathcal{A}_n be the simple adversarial rule outlined above. A very simple VN rule Φ and nested core nominatable sequence \mathbf{F} for which

$$\mathbf{F} = (F_n)_{n=n_0}^\infty \in \mathfrak{C}_{\Phi}^{(k_n)} \implies (f_{\mathcal{A}_n}(F_n))_{n=n_0}^\infty \in \mathfrak{N} \setminus \mathfrak{C}_{\Phi}^{(k_n)}.$$

proceeds as follows. Consider $F_n = \text{SBM}(\rho, n, K, B, \pi)$ supported on $\mathcal{G}_n \times \mathcal{G}_n$ where B is as in Eq. 4 with $\pi = (1/2, 1/2)$, $p > q > r$ fixed, and $\rho > 0$ fixed. Suppose that Φ_n is a VN scheme that runs spectral clustering on the contaminated graph by first selecting the number of communities in a consistent manner (via adjacency spectral clustering for example [27]) and ranking all the vertices in the group with the highest probability of within-group connection (in a fixed but arbitrary order), and then ranks the rest of the vertices in fixed but arbitrary order. Suppose that we consider $k_n = n/2$. It is immediate that $\mathbf{F} = (F_n)_{n=n_0}^\infty \in \mathfrak{C}_{\Phi}^{(k_n)}$ and that the adversary acting on G_2 impacts this consistency. Indeed, if either

1. $p - q < s_-$, or
2. $\frac{p-q}{1-q} < s_+$,

then Φ_n is no longer consistent with respect to the adversarially contaminated model sequence.

4 Experiments

We next explore the effect of our adversarial noise model in a simulated data experiment, and the effect of adversarial contamination and regularization in a real data example derived from Bing entity transition graphs. First, we explain in detail the steps of the VN scheme we will consider in our experiments.

4.1 VN via ASE o GMM

In the contamination model of Section 3.1, we consider the following VN scheme, denoted VN o GMM o ASE. Letting $v^* \in V(G_1)$ (resp., $V^* \subset V(G_1)$) be the vertex (resp., vertices) of interest in G_1 , we seek the corresponding vertex (resp., vertices) of interest in $V(G_2)$ as follows:

1. Given two graphs, G_1 and G_2 , we use Adjacency Spectral Embedding (ASE) [43] to separately embed G_1 and G_2 into a common Euclidean space \mathbb{R}^d . Given the $n \times n$ adjacency matrix A of G_1 , the d -dimensional ASE of G_1 is defined as follows.

Definition 18 (Adjacency spectral embedding (ASE)). Given $d \in \mathbb{Z} > 0$, the *adjacency spectral embedding* (ASE) of A into \mathbb{R}^d is defined via $\widehat{X} = U_A S_A^{1/2}$ where

$$|A| = [U_A | U_A^\perp] [S_A \oplus S_A^\perp] [U_A | U_A^\perp]$$

is the spectral decomposition of $|A| = (A^T A)^{1/2}$, $S_A \in \mathbb{R}^{d \times d}$ is the diagonal matrix with the d largest eigenvalues of $|A|$ on its diagonal and $U_A \in \mathbb{R}^{n \times d}$ has columns which are the eigenvectors corresponding to the eigenvalues of S_A .

Simply stated, the ASE of a graph G provides Euclidean features for each vertex in G on which to perform subsequent inference. Combined with recent efforts to prove that the ASE provides consistent estimators of the latent position parameters in random dot product graphs and positive-definite stochastic blockmodels [43, 2], the ASE allows for a host classical inference methodologies to be successfully employed within these random graph frameworks [44, 45, 28]. To choose d above, we use the machinery of [49, 9] to develop the principled heuristic of estimating d as the larger of the two elbows of the associated scree plots of the singular values of G_1 and G_2 .

2. Solve the orthogonal Procrustes problem [39] to find an orthogonal transformation aligning the seeded vertices across graphs. Let \widehat{X}_S (resp., \widehat{Y}_S) be the matrix composed of the rows of ASE(G_1) (resp., ASE(G_2)) corresponding to the seeded vertices in S . Letting the SVD of $\widehat{Y}_S^T \widehat{X}_S = U \Sigma V^T$, the solution to

$$R = \operatorname{argmin}_{O \text{ s.t. } O^T O = I} \|\widehat{X}_S - \widehat{Y}_S O\|_F,$$

is given by $R = UV^T$. Use this transformation to align the embeddings of G_1 and G_2 in \mathbb{R}^d , i.e., rotate \widehat{Y} via $\widehat{Y}O$ to align \widehat{Y} to \widehat{X} .

3. Motivated by the central limit theorem of [3] for the residual errors between the rows of the ASE and the latent position parameters in random dot product graphs, we use model-based Gaussian mixture modeling (GMM) to simultaneously cluster the vertices of the embedded graphs. Here, we employ the R package `MClust` [18].

4. Rank the candidate matches in G_2 according to the following heuristic. If $u \in V(G_1)$ and $v \in V(G_2)$ are clustered points in the Procrustes-aligned embedding of G_1 and G_2 with respective covariance matrices Σ_u and Σ_v in their components of the GMM, then compute

$$\Delta(u, v) = \max(D_u(u, v), D_v(u, v)),$$

where

$$D_u(u, v) = \sqrt{(u - v)\Sigma_u^{-1}(u - v)^T} \text{ and } D_v(u, v) = \sqrt{(u - v)\Sigma_v^{-1}(u - v)^T}$$

are the respective Mahalanobis distances from u to v . In the case of a single v.o.i. v^* , rank the vertices in G_2 then by increasing value of $\Delta(v^*, u)$, i.e., with ties broken in a fixed deterministic fashion, we rank via (where $n_2 = |V(G_2)|$)

$$\begin{aligned} \Phi_n(g_1, g_2, v^*)[1] &\in \arg \min_{u \in V(G_2)} \Delta(v^*, u) \\ \Phi_n(g_1, g_2, v^*)[2] &\in \arg \min_{u \in V(G_2) \setminus \{\Phi_n[1]\}} \Delta(v^*, u) \\ &\vdots \\ \Phi_n(g_1, g_2, v^*)[n_2 - 1] &\in \arg \min_{u \in V(G_2) \setminus \{\cup_{j \leq n_2 - 2} \Phi_n[j]\}} \Delta(v^*, u) \\ \Phi_n(g_1, g_2, v^*)[n_2] &\in \arg \min_{u \in C_{v^*} \setminus \{\cup_{j \leq n_2 - 1} \Phi_n[j]\}} \Delta(v^*, u). \end{aligned}$$

In the case of multiple v.o.i. V^* , rank the vertices in G_2 then by increasing value of $\min_{v \in V^*} \Delta(v, u)$ with ties broken in a fixed deterministic fashion.

4.2 Simulation

We consider the model in Section 3.1 with the following parameter choices:

$$\begin{aligned} n &= 200; & \pi &= (1/2, 1/2); & \pi_- &= 0.1, & \pi_+ &= 0.1; \\ p &= 0.4; & q &= 0.5; & r &= 0.3; \\ s_+ &= 0.8; & s_- &= 0.8; & \rho &\in (0.3, 0.5, 0.7). \end{aligned}$$

Note that, in the notation of Section 3.1, if $(G_1, G_2) \sim \text{SBM}(\rho, n, K, B, \pi)$, we will consider

$$\begin{aligned} G_1^{(i)} &= G_1[\tilde{B}_1 \cup \tilde{B}_2] \\ G_2^{(i)} &= G_2[\tilde{B}_1 \cup \tilde{B}_2] \\ G_2^{(c)} &= G_2 \text{ acted upon by the adversary described in Section 3.1;} \\ G_2^{(x,y)} &= G_2^{(c)} \text{ trimmed as in Algorithm 1.} \end{aligned}$$

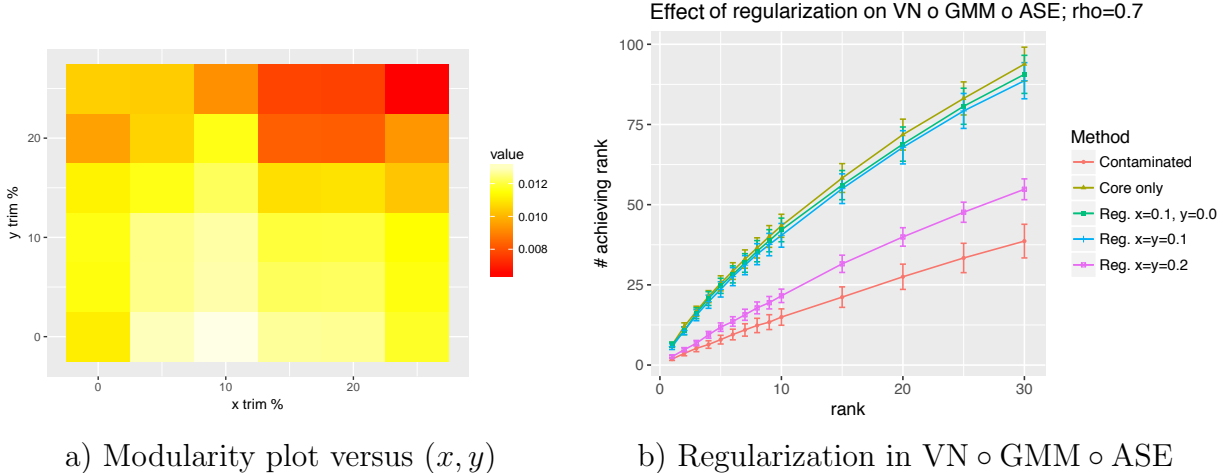
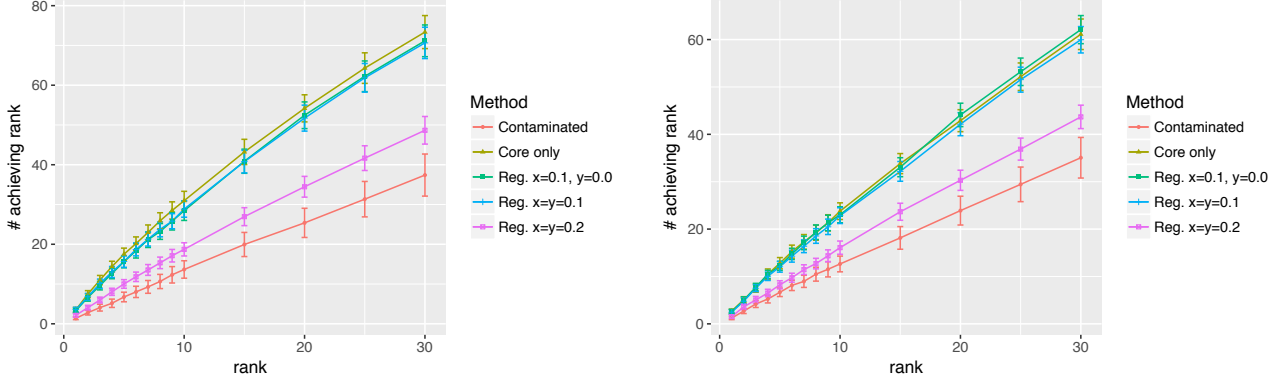


Figure 4: In the left panel, we plot the modularity of the GMM clustering in the trimmed $G_2^{(x,y)}$ as a function of $x, y \in \{0, 0.05, 0.1, 0.15, 0.2, 0.25\}$. Note that we average the modularity values over $nMC = 50$ randomly selected seed sets of size $s = 10$. The color indicates the value of the modularity, with darker red indicating lower values and lighter yellow–white indicating larger values. In the right panel, we plot the performance of $\text{VN} \circ \text{GMM} \circ \text{ASE}$ ($\pm 2\text{s.e.}$) in $(G_1, G_2) \sim \text{SBM}(0.7, 200, 2, B, \pi = (1/2, 1/2))$ again averaged over $nMC = 50$ random seed sets of size $s = 10$. The x -axis shows the ranks in the nomination list and the y -axis shows (on average) how many vertices $v \in G_1^{(i)}$, when viewed as the v.o.i., had their corresponding vertex of interest ranked in the top x by $\text{VN} \circ \text{GMM} \circ \text{ASE}$. The gold line represents performance in the idealized network pair $(G_1^{(i)}, G_2^{(i)})$; the red line for $(G_1^{(i)}, G_2^{(c)})$; the green line for $(G_1^{(i)}, G_2^{(0.1,0)})$; the blue line for $(G_1^{(i)}, G_2^{(0.1,0.1)})$; and the pink line for $(G_1^{(i)}, G_2^{(0.2,0.2)})$.

In this simulation example, we observe that the adversarial contamination model significantly decreases VN performance and that the trimming regularization mitigates this contamination and recovers much of the lost inferential performance.

In Figure 4 we plot the performance of $\text{VN} \circ \text{GMM} \circ \text{ASE}$ over a number of (x, y) trimming pairs (we note that for all correlation/regularized/contaminated/trimmed combinations, mean performance is significantly better than chance and chance normalized plots are omitted). In the left panel, we plot the modularity of the GMM clustering in the trimmed $G_2^{(x,y)}$ as a function of $x, y \in \{0, 0.05, 0.1, 0.15, 0.2, 0.25\}$. Note that we average the modularity values over $nMC = 50$ randomly selected seed sets of size $s = 10$. The color indicates the value of the modularity, with darker red indicating lower values and lighter yellow–white indicating larger values. We see that modularity is maximized near $(x, y) \approx (0.1, 0)$, and that the model-true trimming values $(x, y) = (0.1, 0.1)$ achieves relatively high modularity as well.

In the right panel, we plot the performance of $\text{VN} \circ \text{GMM} \circ \text{ASE}$ ($\pm 2\text{s.e.}$) in $(G_1, G_2) \sim \text{SBM}(0.7, 200, 2, B, \pi = (1/2, 1/2))$ again averaged over $nMC = 50$ random seed sets of size $s = 10$. The x -axis shows the ranks in the nomination list and



a) Regularized VN o GMM o ASE; $\rho = 0.5$ b) Regularized VN o GMM o ASE; $\rho = 0.3$

Figure 5: In the right panel (resp., left panel), we plot the performance of VN o GMM o ASE ($\pm 2s.e.$) in $(G_1, G_2) \sim \text{SBM}(0.3, 200, 2, B, \pi = (1/2, 1/2))$ with $\rho = 0.3$ (resp., $\rho = 0.5$) again averaged over $nMC = 50$ random seed sets of size $s = 10$. The x -axis shows the ranks in the nomination list and the y -axis shows (on average) how many vertices $v \in G_1^{(i)}$, when viewed as the v.o.i., had their corresponding vertex of interest ranked in the top x by VN o GMM o ASE. The gold line represents performance in the idealized network pair $(G_1^{(i)}, G_2^{(i)})$; the red line for $(G_1^{(i)}, G_2^{(c)})$; the green line for $(G_1^{(i)}, G_2^{(0.1,0)})$; the blue line for $(G_1^{(i)}, G_2^{(0.1,0.1)})$; and the pink line for $(G_1^{(i)}, G_2^{(0.2,0.2)})$.

the y -axis shows (on average) how many vertices $v \in G_1^{(i)}$, when viewed as the v.o.i., had their corresponding vertex of interest ranked in the top x by VN o GMM o ASE. The gold line represents performance in the idealized network pair $(G_1^{(i)}, G_2^{(i)})$; the red line for $(G_1^{(i)}, G_2^{(c)})$; the green line for $(G_1^{(i)}, G_2^{(0.1,0)})$; the blue line for $(G_1^{(i)}, G_2^{(0.1,0.1)})$; and the pink line for $(G_1^{(i)}, G_2^{(0.2,0.2)})$. We see here that, as expected, performance loss due to contamination is mitigated by using the true model-based trimming parameters $x = y = 0.1$, and using the modularity maximizing $x = 0.1, y = 0$. If we over-trim, here represented by $x = y = 0.2$, we see a degradation in performance; as expected from the low modularity value in the left panel for $x = y = 0.2$. We again see here the interesting phenomena observed in the motivating high school friendship network example of Section 1.1: modularity and subsequently VN performance tends to emphasize more trimming of the low degree vertices and less trimming of the high degree vertices. This suggests that low-degree contamination is most effective at thwarting the performance on VN o GMM o ASE, perhaps contrary to the intuition that high-degree nodes adversely affect concentration of adjacency matrices [24].

As in our motivating example, trimming can have the effect of removing v.o.i. from $G_2^{(c)}$, and we see this play out in Figure 6. As expected, over-regularizing results in a significant number of v.o.i. being trimmed and significant performance loss as compared to the more moderate choices of regularization. Lastly, exploring the affect

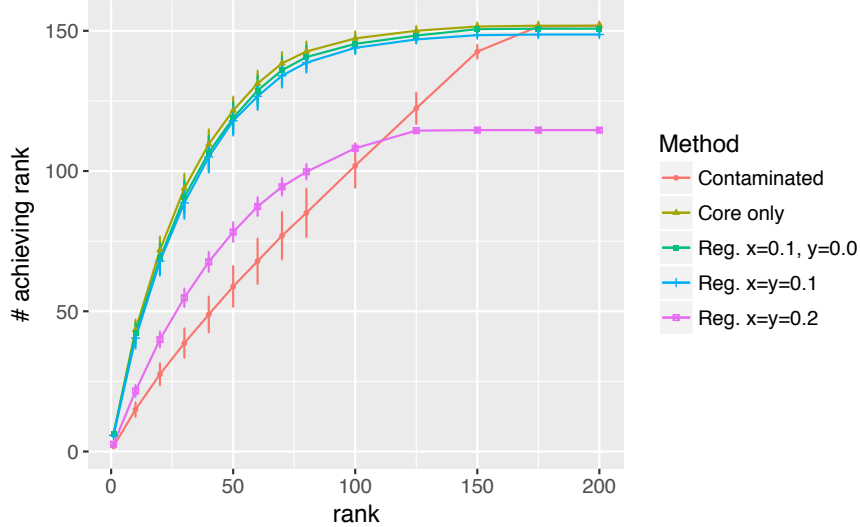


Figure 6: We plot the performance of $\text{VN} \circ \text{GMM} \circ \text{ASE}$ ($\pm 2\text{s.e.}$) in $(G_1, G_2) \sim \text{SBM}(0.3, 200, 2, B, \pi = (1/2, 1/2))$ with $\rho = 0.7$ again averaged over $nMC = 50$ random seed sets of size $s = 10$. The x -axis shows the ranks in the nomination list and the y -axis shows (on average) how many vertices $v \in G_1^{(i)}$, when viewed as the v.o.i., had their corresponding vertex of interest ranked in the top x by $\text{VN} \circ \text{GMM} \circ \text{ASE}$. The gold line represents performance in the idealized network pair $(G_1^{(i)}, G_2^{(i)})$; the red line for $(G_1^{(i)}, G_2^{(c)})$; the green line for $(G_1^{(i)}, G_2^{(0.1,0)})$; the blue line for $(G_1^{(i)}, G_2^{(0.1,0.1)})$; and the pink line for $(G_1^{(i)}, G_2^{(0.2,0.2)})$.

of ρ on $\text{VN} \circ \text{GMM} \circ \text{ASE}$ performance, we repeat the above experiment with $\rho = 0.5$, and $\rho = 0.3$. Results are plotted in Figure 5. As expected, the trends observed in Figure 4 hold here as well, with an across the board performance decrease as ρ decreases.

4.3 Microsoft Bing Entity Graph Transitions

In the next example, we consider a multigraph derived from one month of aggregate Bing entity graph transitions. The multigraph represents entity transitions, and each weighted edge-type of the multigraph represents aggregated signal that capture a transition rate between two entities while browsing. There are multiple ways that a transition between those entities could be made, so we count each aggregated signal separately using the different edge-types in the multigraph: one edge-type represents transitions that were made via a suggestion interface; the other edge-type represents transitions that we made independent of any suggestion interface. As such, one type will have a constrained set of transition probabilities (it can realistically only connect to a subset of the vertices in the graph), while the other will be more “unlimited” in that it may connect to any other entity in the entire graph.

The resulting graphs are symmetric, weighted and loop-free, with $G_1^{(i)}$ containing 13535 vertices and 519389 edges, $G_2^{(i)}$ containing 13535 vertices and 595047 edges, and

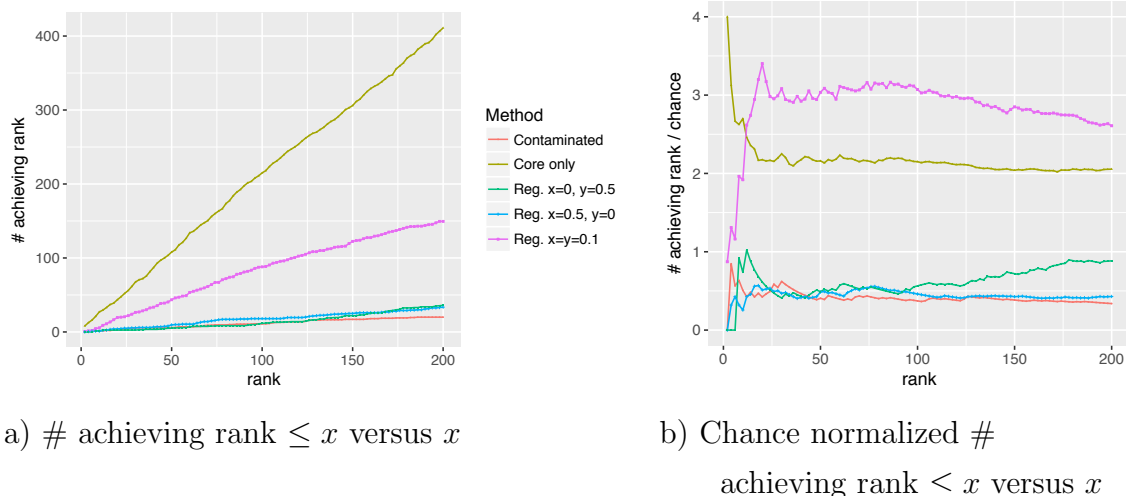


Figure 7: Considering 2 Monte Carlo replicates of $s = 100$ randomly chosen seeds, we run $\text{VN} \circ \text{GMM} \circ \text{ASE}$ on $(G_1^{(i)}, G_2^{(i)})$ (yellow line), on $(G_1^{(i)}, G_2^{(c)})$ (red line), on $(G_1^{(i)}, G_2^{(0.1,0.1)})$ (pink line); on $(G_1^{(i)}, G_2^{(0,0.5)})$ (green line); and on $(G_1^{(i)}, G_2^{(0.5,0)})$ (blue line). In panel a), we consider each vertex in $G_1^{(i)}$ as the v.o.i., and we plot the number of vertices amongst these v.o.i. (x-axis) that had their corresponding v.o.i. in G_2 ranked in the top x . The right panel shows the same result normalized by chance performance, where we plot $y = \frac{\text{mean \# of v.o.i. with corresp. v.o.i. ranked in top } x \text{ by VN} \circ \text{GMM} \circ \text{ASE}}{\text{mean \# of v.o.i. with corresp. v.o.i. ranked in top } x \text{ by chance algorithm}}$ vs. x .

the contaminated network $G_2^{(c)}$ containing 45816 vertices and 2848466 edges. Here, there is a 1-to-1 correspondence between the vertex sets of $G_1^{(i)}$ and $G_2^{(i)}$ with the contaminated network adding 32281 vertices to $G_2^{(c)}$ that do not have a corresponding vertex in $G_1^{(i)}$. In Figure 7, we explore the effect of this contamination (and the subsequent regularization) on $\text{VN} \circ \text{GMM} \circ \text{ASE}$.

Considering two randomly chosen sets of $s = 100$ seeds, we run $\text{VN} \circ \text{GMM} \circ \text{ASE}$ on $(G_1^{(i)}, G_2^{(i)})$ (yellow line in Figure 7), on $(G_1^{(i)}, G_2^{(c)})$ (red line), on $(G_1^{(i)}, G_2^{(0.1,0.1)})$ (pink line); on $(G_1^{(i)}, G_2^{(0,0.5)})$ (green line); and on $(G_1^{(i)}, G_2^{(0.5,0)})$ (blue line). As in the simulations and motivating data example, we see the general trend of contamination adversely affecting performance and regularization ameliorating the effect of the contamination. Here, the regularized graph $G_2^{(0.1,0.1)}$ has 36808 vertices, and as expected, absolute performance (the left panel in Figure 7) in the clean case is better than in the regularized setting. From the right panel, we observe however, that the relative improvement over chance achieved in the regularized setting exceeds that in the clean setting, and we observe that $\text{VN} \circ \text{GMM} \circ \text{ASE}$ performance is worse than chance in the contaminated and over-regularized network settings. While regularization has not recovered the performance in the idealized setting, the improvement induced via regularization is dramatic versus the contaminated setting. We also note that the modularity levels for automating the choice of (x, y) in this example are relatively stable

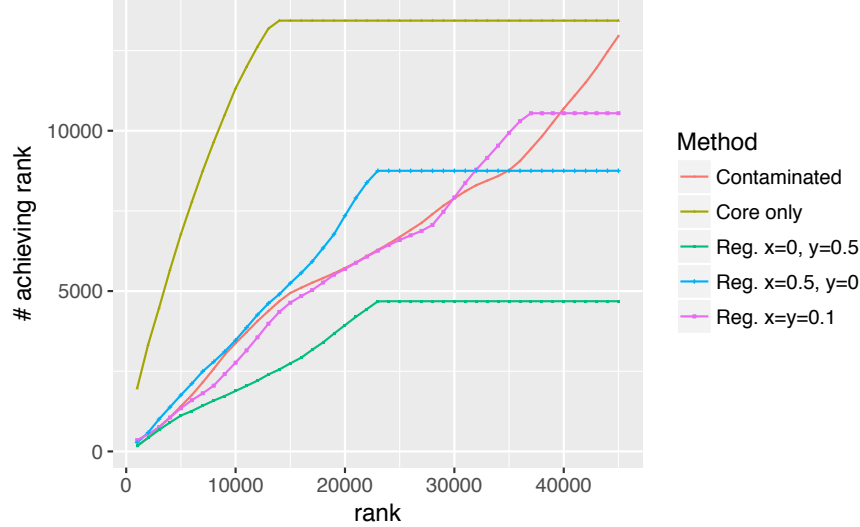


Figure 8: Considering 2 Monte Carlo replicates of $s = 100$ randomly chosen seeds (same seed sets as in Figure 7), we run $\text{VN} \circ \text{GMM} \circ \text{ASE}$ on $(G_1^{(i)}, G_2^{(i)})$ (yellow line), on $(G_1^{(i)}, G_2^{(c)})$ (red line), on $(G_1^{(i)}, G_2^{(0.1,0.1)})$ (pink line); on $(G_1^{(i)}, G_2^{(0,0.5)})$ (green line); and on $(G_1^{(i)}, G_2^{(0.5,0)})$ (blue line). In panel a), we consider each vertex in $G_1^{(i)}$ as the v.o.i., and we plot the number of vertices amongst these v.o.i. (x-axis) that had their corresponding v.o.i. in G_2 ranked in the top x .

to the trimming value, with the clustered $G_2^{(c)}$ achieving $Q = 0.52$, the clustered $G_2^{(c)}$ achieving $Q = 0.52$, the clustered $G_2^{(0,0.5)}$ achieving $Q = 0.57$, the clustered $G_2^{(0.5,0)}$ achieving $Q = 0.52$, and the clustered $G_2^{(0.1,0.1)}$ achieving $Q = 0.53$. Indeed, in this data example the graphs do not cluster particularly well under any trimming conditions, and a more modest trimming scheme is more effective for the subsequent VN inference task.

In Figure 8, we again consider the performance of $\text{VN} \circ \text{GMM} \circ \text{ASE}$ with the same $nMC = 2$ randomly chose 100 vertex seed sets and various levels of regularization, here plotting over an extended x -axis. In pink we plot $\text{VN} \circ \text{GMM} \circ \text{ASE}$ run on $(G_1^{(i)}, G_2^{(0.1,0.1)})$; in blue on $(G_1^{(i)}, G_2^{(0.5,0)})$; in green on $(G_1^{(i)}, G_2^{(0,0.5)})$; and in red on $(G_1^{(i)}, G_2^{(c)})$. This figure demonstrates another dramatic side effect of over-regularization: v.o.i. that are trimmed for $G_2^{(c)}$ can never be recovered by $\text{VN} \circ \text{GMM} \circ \text{ASE}$. This is represented by the horizontal asymptotes in Figure 8.

5 Discussion

Our motivating question is two-fold: What effect does adversarial contamination have on the performance of vertex nomination; and can (statistically) successful vertex nomination be retained in the presence or absence of unmatchable vertices? Herein, we have

demonstrated both theoretically and empirically that an adversary can cause our VN scheme to fail (i.e., nominate the wrong vertices). Empirically, we have also demonstrated that regularization can be effective for mitigating the effect of the contamination model posited herein. Establishing the theoretical effect of regularization on VN is an open problem, and the subject of our present research.

In [26], the authors showed that there can be no universally consistent vertex nomination scheme assuming only one vertex of interest. In this paper, we have seen that with a suitable definition of a maximal consistency class and (possibly) multiple vertices of interest, there are infinitely many such consistency classes, which implies that ensemble methods cannot recover consistency and/or thwart an arbitrary adversary. This allows us to formulate our model of adversarial contamination in terms of consistency classes; indeed, an adversary for a particular VN rule aims to move the distribution out of the rule’s consistency class. A natural next question to consider would be what effect regularization has on a VN rule’s consistency class. Ideally, regularization enlarges the consistency class of a VN rule thereby making the adversary’s job (i.e., moving the model out of the consistency class) more difficult. The interplay between the adversary and regularization in VN is central to this story, although we are only at the infancy of understanding it.

Our proposed definition of an adversary is suited to a general random graph setting, and it provides a simple surrogate in which to study the effect of contamination in real data examples. From our simulation study and real data examples we have seen that a particular VN rule ($\text{VN} \circ \text{GMM} \circ \text{ASE}$) succeeds before adversarial contamination, fails after contamination, and succeeds after graph regularization. We are currently exploring the effect of contamination on a broader class of VN rules, and considering other models for adversarial contamination and subsequent regularization. Finally, while we have partially answered in the negative our question about whether consistency can be retained in the general adversarial setting, another valid consideration is whether there are adversarial models for which the adversary does *not* affect consistency. While we believe even simple manipulation on the edges of G_2 can affect consistency, it may be possible to derive bounds and phase transitions on the number of edges (or vertices) that an adversary would need to modify to change the result. Mathematically, this is akin to finding limits on the size of $|V_{\mathcal{A}}|$ in our definition of an adversary.

A Construction of the Bayes optimal scheme

Given the notation of Section 2, we now develop the Bayes optimal nomination scheme. Let n, m be fixed and let $V^* \subset V_1 \cap V_2$ be fixed. Let W be an obfuscating set and $\mathfrak{o} \in \mathfrak{D}_W$. Define $\mathcal{G}_n^a \times \mathcal{G}_m^a$ to be the set of graphs

$$\mathcal{G}_n^a \times \mathcal{G}_m^a := \{(g_1, g_2) \in \mathcal{G}_n \times \mathcal{G}_m \text{ s.t. } \mathcal{I}(v; g_2) = \{v\} \text{ for all } v \in V^*\}$$

For each $(g_1, g_2) \in \mathcal{G}_n^a \times \mathcal{G}_m^a$ define

$$\begin{aligned} (g_1, [\mathfrak{o}(g_2)]) &= \left\{ (g_1, \tilde{g}_2) \in \mathcal{G}_n^a \times \mathcal{G}_m^a : \mathfrak{o}(\tilde{g}_2) \simeq \mathfrak{o}(g_2) \right\} \\ &= \left\{ (g_1, \tilde{g}_2) \in \mathcal{G}_n^a \times \mathcal{G}_m^a : \tilde{g}_2 \simeq g_2 \right\}. \end{aligned}$$

where \simeq denotes graph isomorphism. For each $w \in W$ and $u \in V_2$, we also define the following restriction

$$\begin{aligned} (g_1, [\mathfrak{o}(g_2)])_{w=\mathfrak{o}(u)} &= \left\{ (g_1, \tilde{g}_2) \in \mathcal{G}_n^a \times \mathcal{G}_m^a : \mathfrak{o}(\tilde{g}_2) = \sigma(\mathfrak{o}(g_2)), \sigma \text{ an isomorphism, } \sigma(w) = \mathfrak{o}(u) \right\} \\ &= \left\{ (g_1, \tilde{g}_2) \in \mathcal{G}_n^a \times \mathcal{G}_m^a : \tilde{g}_2 = \sigma(g_2), \sigma \text{ an isomorphism, } \sigma(\mathfrak{o}^{-1}(w)) = u \right\}, \end{aligned}$$

and for $S \subset V_2$, define

$$(g_1, [\mathfrak{o}(g_2)])_{w \in \mathfrak{o}(S)} = \bigcup_{u \in S} (g_1, [\mathfrak{o}(g_2)])_{w=\mathfrak{o}(u)}.$$

Choose graphs

$$\mathbf{g} = \left\{ \left(g_1^{(i)}, g_2^{(i)} \right) \right\}_{i=1}^h \quad (7)$$

so that the sets

$$\left\{ \left(g_1^{(i)}, [\mathfrak{o}(g_2^{(i)})] \right) \right\}_{i=1}^h$$

partition $\mathcal{G}_n^a \times \mathcal{G}_m^a$. To ease notation, we will denote this partition via $\mathcal{P}_{n,m}^{\mathbf{g}}$. For $F_{c,\theta}^{(n,m)} \in \mathcal{N}$ supported on $\mathcal{G}_n^a \times \mathcal{G}_m^a$, we will next define a Bayes optimal scheme Φ^* (optimal under both loss functions simultaneously for all $k \in [m-1]$). For each $i \in [h]$, set (where ties are broken in a fixed but arbitrary manner)

$$\begin{aligned} \Phi^*(g_1^{(i)}, \mathfrak{o}(g_2^{(i)}), V^*)[1] &\in \arg \max_{u \in W} \mathbb{P}_{F_{c,\theta}^{(n,m)}} \left((g_1^{(i)}, [\mathfrak{o}(g_2^{(i)})])_{u \in \mathfrak{o}(V^*)} \mid (g_1^{(i)}, [\mathfrak{o}(g_2^{(i)})]) \right) \\ \Phi^*(g_1^{(i)}, \mathfrak{o}(g_2^{(i)}), V^*)[2] &\in \arg \max_{u \in W \setminus \{\Phi^*[1]\}} \mathbb{P}_{F_{c,\theta}^{(n,m)}} \left((g_1^{(i)}, [\mathfrak{o}(g_2^{(i)})])_{u \in \mathfrak{o}(V^*)} \mid (g_1^{(i)}, [\mathfrak{o}(g_2^{(i)})]) \right) \\ &\vdots \\ \Phi^*(g_1^{(i)}, \mathfrak{o}(g_2^{(i)}), V^*)[m] &\in \arg \max_{u \in W \setminus \{\cup_{j < m} \Phi^*[j]\}} \mathbb{P}_{F_{c,\theta}^{(n,m)}} \left((g_1^{(i)}, [\mathfrak{o}(g_2^{(i)})])_{u \in \mathfrak{o}(V^*)} \mid (g_1^{(i)}, [\mathfrak{o}(g_2^{(i)})]) \right), \end{aligned}$$

For each element

$$(g_1, g_2) \in (g_1^{(i)}, [\mathfrak{o}(\tilde{g}_2^{(i)})]) \setminus \{(g_1^{(i)}, g_2^{(i)})\},$$

choose an isomorphism σ such that $\mathfrak{o}(g_2) = \sigma(\mathfrak{o}(g_2^{(i)}))$, and define

$$\Phi^*(g_1, \mathfrak{o}(g_2), V^*) = \sigma(\Phi^*(g_1^{(i)}, \mathfrak{o}(g_2^{(i)}), V^*)).$$

For each $i \in [h]$, $j \in [m]$, $v \in V^*$, $\Phi \in \mathcal{V}_{nm}$, define

$$\begin{aligned} U_{i, \mathbf{g}}^{j, v} &:= \left\{ (g_1, g_2) \in \left(g_1^{(i)}, [\mathfrak{o}(g_2^{(i)})] \right) \text{ s.t. } \text{rank}_{\Phi(g_1, \mathfrak{o}(g_2), V^*)}(\mathfrak{o}(v)) = j \right\} \\ &= \left\{ (g_1, g_2) \in \left(g_1^{(i)}, [\mathfrak{o}(g_2^{(i)})] \right) \text{ s.t. } \Phi(g_1, \mathfrak{o}(g_2), V^*)[j] = \mathfrak{o}(v) \right\} \\ &= \left\{ (g_1, g_2) \in \left(g_1^{(i)}, [\mathfrak{o}(g_2^{(i)})] \right) \text{ s.t. } \exists \text{ iso. } \sigma \text{ s.t. } \sigma(\mathfrak{o}(g_2^{(i)})) = \mathfrak{o}(g_2) \text{ and} \right. \\ &\quad \left. \sigma \left(\Phi(g_1^{(i)}, \mathfrak{o}(g_2^{(i)}), V^*)[j] \right) = \mathfrak{o}(v) \right\} \\ &= \left(g_1^{(i)}, [\mathfrak{o}(g_2^{(i)})] \right)_{\Phi(g_1^{(i)}, \mathfrak{o}(g_2^{(i)}), V^*)[j] = \mathfrak{o}(v)}. \end{aligned}$$

Lastly, for $(g_1, g_2) \in \mathcal{G}_n^a \times \mathcal{G}_m^a$, define $p_\Phi \in [0, 1]^m$ via

$$\begin{aligned} p_\Phi^{(i)}[g_1, \mathfrak{o}(g_2), V^*][j] &= p_\Phi^{(i)}[j] := \sum_{v \in V^*} \mathbb{P}_{F_{c, \theta}^{(n, m)}} \left[U_{i, \mathbf{g}}^{j, v} \mid (g_1^{(i)}, [\mathfrak{o}(g_2^{(i)})]) \right] \\ &= \mathbb{P}_{F_{c, \theta}^{(n, m)}} \left[(g_1, [\mathfrak{o}(g_2)])_{\Phi(g_1, \mathfrak{o}(g_2), V^*)[j] \in \mathfrak{o}(V^*)} \mid (g_1^{(i)}, [\mathfrak{o}(g_2^{(i)})]) \right] \end{aligned}$$

Note that, by definition, p_{Φ^*} majorizes p_Φ .

To show that Φ^* is Bayes optimal for $L_k^{(1)}$ (the proof for $L_k^{(2)}$ being completely analogous), we have that for $k \leq m - 1$,

$$\begin{aligned} L_k^{(1)}(\Phi, V^*) &= 1 - \frac{1}{|V^*|} \sum_{v \in V^*} \mathbb{P}_{F_{c, \theta}^{(n, m)}}(\text{rank}_{\Phi(G_1, \mathfrak{o}(G_2), V^*)}(\mathfrak{o}(v)) \leq k) \\ &= 1 - \frac{1}{|V^*|} \sum_{v \in V^*} \sum_{j \leq k} \mathbb{P}_{F_{c, \theta}^{(n, m)}}(\text{rank}_{\Phi(G_1, \mathfrak{o}(G_2), V^*)}(\mathfrak{o}(v)) = j) \\ &= 1 - \frac{1}{|V^*|} \sum_{\mathcal{P}_{\mathbf{g}}} \sum_{j \leq k} \sum_{v \in V^*} \mathbb{P}_{F_{c, \theta}^{(n, m)}} \left[U_{i, \mathbf{g}}^{j, v} \mid (g_1^{(i)}, [\mathfrak{o}(g_2^{(i)})]) \right] \mathbb{P}_{F_{c, \theta}^{(n, m)}} \left[(g_1^{(i)}, [\mathfrak{o}(g_2^{(i)})]) \right] \\ &= 1 - \frac{1}{|V^*|} \sum_{\mathcal{P}_{\mathbf{g}}} \sum_{j \leq k} p_\Phi^{(i)}[j] \mathbb{P}_{F_{c, \theta}^{(n, m)}} \left[(g_1^{(i)}, [\mathfrak{o}(g_2^{(i)})]) \right] \\ &\geq 1 - \frac{1}{|V^*|} \sum_{\mathcal{P}_{\mathbf{g}}} \sum_{j \leq k} p_{\Phi^*}^{(i)}[j] \mathbb{P}_{F_{c, \theta}^{(n, m)}} \left[(g_1^{(i)}, [\mathfrak{o}(g_2^{(i)})]) \right] \\ &= L_k^{(1)}(\Phi^*, V^*), \end{aligned}$$

as desired.

B Proof of Lemma 11

We first note that the growth condition on $|V_n^*|$ and on k_n in the precision case ensures that the result for precision and recall consistency follow from each other, and so we will focus our attention on recall consistency. The analogous result for precision follows *mutatis mutandis*.

Consider the following network construction for a network of size n . Let $\xi_n = \max(k_n, |V_n^*|)$. For a fixed $p \in (0, 1)$, let $B_1, \dots, B_{\lfloor \frac{n/3}{\xi_n} \rfloor}$ be i.i.d. $\text{ER}(\xi_n, p)$ random graphs. Let H_n be a complete graph on $n - \xi_n \lfloor \frac{n/3}{\xi_n} \rfloor$ vertices. Label the vertices

- of B_i with $\{1, 2, 3, \dots, \xi_n\}$;
- of B_2 with $\{\xi_n + 1, \xi_n + 2, \xi_n + 3, \dots, 2\xi_n\}$;
- ⋮
- of B_{i-1} with $\{(i-2)\xi_n + 1, (i-2)\xi_n + 2, (i-2)\xi_n + 3, \dots, (i-1)\xi_n\}$;
- of B_1 with $\{(i-1)\xi_n + 1, (i-1)\xi_n + 2, (i-1)\xi_n + 3, \dots, i\xi_n\}$;
- of B_{i+1} with $\{i\xi_n + 1, i\xi_n + 2, i\xi_n + 3, \dots, (i+1)\xi_n\}$;
- ⋮
- of $B_{\lfloor \frac{n/3}{\xi_n} \rfloor}$ with $\left\{ \left(\left\lfloor \frac{n/3}{\xi_n} \right\rfloor - 1 \right) \xi_n + 1, \left(\left\lfloor \frac{n/3}{\xi_n} \right\rfloor - 1 \right) \xi_n + 2, \dots, \left\lfloor \frac{n/3}{\xi_n} \right\rfloor \xi_n \right\}$;
- of H_n with $\left\{ \left\lfloor \frac{n/3}{\xi_n} \right\rfloor \xi_n + 1, \left\lfloor \frac{n/3}{\xi_n} \right\rfloor \xi_n + 2, \dots, n \right\}$.

For each $\ell \in \left[\left\lfloor \frac{n/3}{\xi_n} \right\rfloor \right]$ and each vertex v in $V(B_\ell)$, independent of all other edges in the network, select ℓ vertices uniformly at random from H_n , i.e., from

$$\left\{ \left\lfloor \frac{n/3}{\xi_n} \right\rfloor \xi_n + 1, \left\lfloor \frac{n/3}{\xi_n} \right\rfloor \xi_n + 2, \dots, n \right\}.$$

Denote this set of ℓ vertices via $V_{v,\ell}$ —and place an edge between v and each vertex in $V_{v,\ell}$. Let $\mathcal{H}_{n,i}$ be the collection of all graphs possible under the above construction, and let $F_{n,i}$ be the distribution on $\mathcal{H}_{n,i}$ outlined above.

With $c = n$, the correspondence the identity, and (where $|V_n^*| = \nu_n$) $V_n^* = \{v_i\}_{i=1}^{\nu_n} = \{u_i\}_{i=1}^{\nu_n} = [\nu_n]$, define the collection of nominatable distributions

$$\left\{ \tilde{F}_{n,i} \right\}_{i=1}^{\lfloor \frac{n/3}{\xi_n} \rfloor}$$

via $\tilde{F}_{n,i} = F_{n,1} \times F_{n,i}$ (where “ \times ” denotes the usual product measure).

Suppose a VN rule $\Phi = (\Phi_n)_{n=n_0}^\infty$ is level- (k_n) recall consistent for $\mathbf{F}_i = (\tilde{F}_{n,i})_{n=n_0}^\infty$. Then, by definition

$$\lim_{n \rightarrow \infty} L_{k_n}^{(1)}(\Phi_n, V^*) - L_{k_n}^{*,(1)}(V^*, \tilde{F}_{n,i}) = 0.$$

However, note that here

$$L_{k_n}^{*,(1)}(V^*, \tilde{F}_{n,i}) \leq 1 - \frac{k_n}{\xi_n}.$$

Indeed, for a given $\tilde{F}_{n,i}$, consider the following VN scheme Ψ_n . First identify the vertices of H_n ; this is possible as H_n is a complete subgraph of order $\geq 2n/3$, and each B_i is of order $o(n)$ with vertices of degree at most $\lfloor \frac{n/3}{\xi_n} \rfloor \leq n/3$. Each B_ℓ can then be recovered and identified by computing the number of edges between H_n and each vertex $v \in V \setminus V(H_n)$; in particular B_i can be identified as the set of vertices in $V \setminus V(H_n)$ with i edges to $V(H_n)$. Let ψ_n then rank the vertices in B_i (in arbitrary order) at the top of its nomination list. It is immediate then that

$$L_{k_n}^{(1)}(\Psi_n, V^*) = 1 - \frac{k_n}{\xi_n}.$$

By the distributional symmetry of the v.o.i., we have that for $v \in V^*$,

$$\mathbb{P}_{\tilde{F}_{n,i}}(\text{rank}_{\Phi_n(G_1, \sigma(G_2), V^*)}(\sigma(v)) \geq k_n + 1) = L_{k_n}^{(1)}(\Phi_n, V^*).$$

For any $\epsilon > 0$ and sufficiently large n , consistency ensures that

$$\mathbb{P}_{\tilde{F}_{n,i}}(\text{rank}_{\Phi_n(G_1, \sigma(G_2), V^*)}(\sigma(v)) \geq k_n + 1) \leq \epsilon + \left(1 - \frac{k_n}{\xi_n}\right).$$

The internal consistency criterion in the definition of VN schemes (Eq. 1), then implies that

$$\mathbb{P}_{\tilde{F}_{n,i}}(\text{rank}_{\Phi_n(G_1, \sigma(G_2), V^*)}(\sigma(v)) \geq k_n + 1) \leq \epsilon + \left(1 - \frac{k_n}{\xi_n}\right) \quad (8)$$

for each $v \in \{1, 2, \dots, \xi_n\}$. Now, suppose that Φ is also level- k_n recall consistent for \mathbf{F}_j for $j \neq i$. By similar logic, we must have that

$$\mathbb{P}_{\tilde{F}_{n,j}}(\text{rank}_{\Phi_n(G_1, \sigma(G_2), V^*)}(\sigma(v)) \geq k_n + 1) \leq \epsilon + \left(1 - \frac{k_n}{\xi_n}\right) \quad (9)$$

for each $v \in \{1, 2, \dots, \xi_n\}$ for sufficiently large n .

Let $\sigma_{i \leftrightarrow j}$ be the permutation on $\{1, \dots, n\}$ defined as

$$\sigma(\ell) := \begin{cases} (i-1)\xi_n + \ell & \ell \in \{1, 2, \dots, \xi_n\} \\ \ell - (j-1)\xi_n & \ell \in \{(j-1)\xi_n + 1, \dots, j\xi_n\} \\ (j-i)\xi_n + \ell & \ell \in \{(i-1)\xi_n + 1, \dots, i\xi_n\} \\ \ell & \text{otherwise.} \end{cases}$$

Now, for each $v \in [\xi_n]$, define the sets

$$\begin{aligned} E_{n,i}^v &:= \{(g_1, g_2) \in \mathcal{H}_{n,1} \times \mathcal{H}_{n,i} : \text{rank}_{\Phi_n(g_1, \sigma(g_2), V_n^*)}(\sigma(v)) \leq k_n\} \\ B_{n,i,j}^v &:= \{(g_1, g_2) \in \mathcal{H}_{n,1} \times \mathcal{H}_{n,i} : \text{rank}_{\Phi_n(g_1, \sigma(g_2), V_n^*)}(\sigma[(j-1)\xi_n + v]) \leq k_n\} \\ E_{n,j}^v &:= \{(g_1, g_2) \in \mathcal{H}_{n,1} \times \mathcal{H}_{n,j} : \text{rank}_{\Phi_n(g_1, \sigma(g_2), V_n^*)}(\sigma(v)) \leq k_n\} \end{aligned}$$

By consistency with respect to $\tilde{F}_{n,i}$ and $\tilde{F}_{n,j}$, i.e., by Eqs. 8–9, we have that for any $\epsilon > 0$, there exists \tilde{n} such that for $n \geq \tilde{n}$, we have

$$\mathbb{P}_{\tilde{F}_{n,i}}(E_{n,i}^v) \geq \frac{k_n}{\xi_n} - \epsilon; \quad (10)$$

$$\mathbb{P}_{\tilde{F}_{n,j}}(E_{n,j}^v) \geq \frac{k_n}{\xi_n} - \epsilon.$$

As $(G_1, G_2) \sim \tilde{F}_{n,i} \Leftrightarrow (G_1, \sigma(G_2)) \sim \tilde{F}_{n,j}$, the internal consistency criterion (Eq. 1) of a VN scheme then implies that

$$\mathbb{P}_{\tilde{F}_{n,j}}(E_{n,j}^v) = \mathbb{P}_{\tilde{F}_{n,i}}(B_{n,i,j}^v) \geq \frac{k_n}{\xi_n} - \epsilon. \quad (11)$$

Now, for each $v \in [\xi_n]$ and $h \in [k_n]$ define

$$\alpha_{v,h} = \mathbb{P}_{\tilde{F}_{n,i}} \left[\underbrace{(g_1, g_2) \in \mathcal{H}_{n,1} \times \mathcal{H}_{n,i} : \text{rank}_{\Phi_n(g_1, \sigma(g_2), V_n^*)}(\mathfrak{o}(v)) = h}_{R_{i,v,h}} \right]$$

$$\beta_{v,h} = \mathbb{P}_{\tilde{F}_{n,i}} \left[\underbrace{(g_1, g_2) \in \mathcal{H}_{n,1} \times \mathcal{H}_{n,i} : \text{rank}_{\Phi_n(g_1, \sigma(g_2), V_n^*)}(\mathfrak{o}[(j-1)\xi_n + v]) = h}_{S_{i,v,h}} \right].$$

By Eq. 10, we have that $\sum_{h=1}^{k_n} \alpha_{v,h} \geq \frac{k_n}{\xi_n} - \epsilon$, and by Eq. 11, we have that $\sum_{h=1}^{k_n} \beta_{v,h} \geq \frac{k_n}{\xi_n} - \epsilon$. Noting that for each $h \in [k_n]$

$$\begin{aligned} 1 &\geq \mathbb{P}_{\tilde{F}_{n,i}} \left[\left(\bigcup_{v \in [\xi_n]} R_{i,v,h} \right) \cup \left(\bigcup_{v \in [\xi_n]} S_{i,v,h} \right) \right] \\ &= \sum_{v \in [\xi_n]} \mathbb{P}_{\tilde{F}_{n,i}}(R_{i,v,h}) + \mathbb{P}_{\tilde{F}_{n,i}}(S_{i,v,h}) \\ &= \xi_n \alpha_{v,h} + \xi_n \beta_{v,h}, \end{aligned}$$

and hence

$$\beta_{v,h} \leq \frac{1}{\xi_n} - \alpha_{v,h}.$$

Plugging this into Eq. 11 then yields

$$\begin{aligned} \frac{k_n}{\xi_n} - \epsilon &\leq \mathbb{P}_{\tilde{F}_{n,i}}(B_{n,i,j}^v) \\ &= \sum_{h=1}^{k_n} \beta_{v,h} \\ &\leq \frac{k_n}{\xi_n} - \sum_{h=1}^{k_n} \alpha_{v,h} \\ &\leq \epsilon. \end{aligned}$$

As ϵ was chosen arbitrarily, and $\frac{k_n}{\xi_n}$ is bounded away from 0 by assumption, we reach our desired contradiction, and Φ cannot be consistent with respect to both \mathbf{F}_i and \mathbf{F}_j . As $i, j \in \lfloor \frac{n_0/3}{\xi_{n_0}} \rfloor$ were arbitrary, we see that there must be at least countably many consistency classes (since there are at least $\lfloor \frac{n_0/3}{\xi_{n_0}} \rfloor$ and we can let n_0 tend to infinity).

References

- [1] J. D Arroyo-Reli3n, D. Kessler, E. Levina, and S. F. Taylor. Network classification with applications to brain connectomics. *arXiv preprint arXiv:1701.08140*, 2017.
- [2] A. Athreya, D. E. Fishkind, K. Levin, V. Lyzinski, Y. Park, Y. Qin, D. L. Sussman, M. Tang, J. T. Vogelstein, and C. E. Priebe. Statistical inference on random dot product graphs: a survey. *ArXiv e-prints*, September 2017.
- [3] A. Athreya, C.E. Priebe, M. Tang, V. Lyzinski, D.J. Marchette, and D.L. Sussman. A limit theorem for scaled eigenvectors of random dot product graphs. *Sankhya A*, pages 1–18, 2015.
- [4] P. J. Bickel and A. Chen. A nonparametric view of network models and Newman-Girvan and other modularities. *Proc. National Academy of Sciences, USA*, 106:21068–21073, 2009.
- [5] P. J. Bickel, D. Choi, X. Chang, and H. Zhang. Asymptotic normality of maximum likelihood and its variational approximation for stochastic blockmodels. *The Annals of Statistics*, 41(4):1922–1943, 2013.
- [6] V. D. Blondel, J.-L. Guillaume, R. Lambiotte, and E. Lefebvre. Fast unfolding of communities in large networks. *Journal of Statistical Mechanics: Theory and Experiment*, 2008.
- [7] E. Bullmore and O. Sporns. Complex brain networks: graph theoretical analysis of structural and functional systems. *Nature Reviews Neuroscience*, 10(3):186, 2009.
- [8] T. T. Cai and X. Li. Robust and computationally feasible community detection in the presence of arbitrary outlier nodes. *The Annals of Statistics*, 43(3):1027–1059, 2015.
- [9] S. Chatterjee. Matrix estimation by universal singular value thresholding. *The Annals of Statistics*, 43(1):177–214, 2014.
- [10] L. Chen, C. Shen, J. T. Vogelstein, and C. E. Priebe. Robust vertex classification. *IEEE transactions on pattern analysis and machine intelligence*, 38(3):578–590, 2016.
- [11] D. Conte, P. Foggia, C. Sansone, and M. Vento. Thirty years of graph matching in pattern recognition. *International Journal of Pattern Recognition and Artificial Intelligence*, 18(03):265–298, 2004.
- [12] G. Coppersmith. Vertex nomination. *Wiley Interdisciplinary Reviews: Computational Statistics*, 6(2):144–153, 2014.

- [13] G. A. Coppersmith and C. E. Priebe. Vertex nomination via content and context. *arXiv preprint arXiv:1201.4118*, 2012.
- [14] H. Dai, H. Li, T. Tian, X. Huang, L. Wang, J. Zhu, and L. Song. Adversarial Attack on Graph Structured Data. *ArXiv e-prints*, June 2018.
- [15] D. Edge, J. Larson, M. Mobius, and C. White. Trimming the hairball: Edge cutting strategies for making dense graphs usable. In *2018 IEEE International Conference on Big Data (Big Data)*, pages 3951–3958. IEEE, 2018.
- [16] D. E. Fishkind, V. Lyzinski, H. Pao, L. Chen, and C. E. Priebe. Vertex nomination schemes for membership prediction. *The Annals of Applied Statistics*, 9(3):1510–1532, 2015.
- [17] P. Foggia, G. Percannella, and M. Vento. Graph matching and learning in pattern recognition in the last 10 years. *International Journal of Pattern Recognition and Artificial Intelligence*, 28(01):1450001, 2014.
- [18] C. Fraley and A. E. Raftery. Mclust: Software for model-based cluster analysis. *Journal of Classification*, 16(2):297–306, 1999.
- [19] K. J. Gile and M. S. Handcock. 7. respondent-driven sampling: An assessment of current methodology. *Sociological methodology*, 40(1):285–327, 2010.
- [20] M. Girvan and M. E. J. Newman. Community structure in social and biological networks. *Proceedings of the national academy of sciences*, 99(12):7821–7826, 2002.
- [21] D. D. Heckathorn. Respondent-driven sampling: a new approach to the study of hidden populations. *Social problems*, 44(2):174–199, 1997.
- [22] P. W. Holland, K. B. Laskey, and S. Leinhardt. Stochastic blockmodels: First steps. *Social networks*, 5(2):109–137, 1983.
- [23] L. Huang, A. D. Joseph, B. Nelson, B. I. P. Rubinstein, and J. D. Tygar. Adversarial machine learning. In *Proceedings of the 4th ACM workshop on Security and artificial intelligence*, pages 43–58. ACM, 2011.
- [24] C. M. Le, E. Levina, and R. Vershynin. Concentration and regularization of random graphs. *Random Structures & Algorithms*, 51(3):538–561, 2017.
- [25] D. S. Lee and C. E. Priebe. Bayesian vertex nomination. *arXiv preprint arXiv:1205.5082*, 2012.
- [26] V. Lyzinski, K. Levin, and C. E. Priebe. On consistent vertex nomination schemes. *Journal of Machine Learning Research*, to appear, 2019.

- [27] V. Lyzinski, D. L. Sussman, M. Tang, A. Athreya, and C. E. Priebe. Perfect clustering for stochastic blockmodel graphs via adjacency spectral embedding. *Electronic Journal of Statistics*, 8:2905–2922, 2014.
- [28] V. Lyzinski, M. Tang, A. Athreya, Y. Park, and C. E. Priebe. Community detection and classification in hierarchical stochastic blockmodels. *IEEE Transactions on Network Science and Engineering*, 4(1):13–26, 2017.
- [29] D. Marchette, C. E. Priebe, and G. Coppersmith. Vertex nomination via attributed random dot product graphs. In *Proceedings of the 57th ISI World Statistics Congress*, volume 6, page 16, 2011.
- [30] S. Maslov and K. Sneppen. Specificity and stability in topology of protein networks. *Science*, 296(5569):910–913, 2002.
- [31] R. Mastrandrea, J. Fournet, and A. Barrat. Contact patterns in a high school: a comparison between data collected using wearable sensors, contact diaries and friendship surveys. *PloS one*, 10(9):e0136497, 2015.
- [32] R. Milo, S. Shen-Orr, S. Itzkovitz, . Kashtan, D. Chklovskii, and U. Alon. Network motifs: simple building blocks of complex networks. *Science*, 298(5594):824–827, 2002.
- [33] M. E. J. Newman. Modularity and community structure in networks. *Proceedings of the National Academy of Sciences*, 103(23):8577–8582, 2006.
- [34] M. E. J. Newman, D. J. Watts, and S. H. Strogatz. Random graph models of social networks. *Proceedings of the National Academy of Sciences*, 99(suppl 1):2566–2572, 2002.
- [35] N. Papernot, P. McDaniel, S. Jha, M. Fredrikson, Z. B. Celik, and A. Swami. The limitations of deep learning in adversarial settings. In *Security and Privacy (EuroS&P), 2016 IEEE European Symposium on*, pages 372–387. IEEE, 2016.
- [36] H. G. Patsolic, Y. Park, V. Lyzinski, and C. E. Priebe. Vertex nomination via local neighborhood matching. *arXiv preprint arXiv:1705.00674*, 2017.
- [37] T. Qin and K. Rohe. Regularized spectral clustering under the degree-corrected stochastic blockmodel. *Advances in Neural Information Processing Systems*, 2013.
- [38] K. Rohe, S. Chatterjee, and B. Yu. Spectral clustering and the high-dimensional stochastic blockmodel. *Annals of Statistics*, 39:1878–1915, 2011.
- [39] P. H. Schönemann. A generalized solution of the orthogonal procrustes problem. *Psychometrika*, 31(1):1–10, 1966.
- [40] J. Scott. *Social network analysis*. Sage, 2017.

- [41] O. Sporns. Graph theory methods: applications in brain networks. *Dialogues in Clinical Neuroscience*, 20(2):111, 2018.
- [42] Stephen M Stigler. The asymptotic distribution of the trimmed mean. *The Annals of Statistics*, pages 472–477, 1973.
- [43] D. L. Sussman, M. Tang, and C. E. Priebe. Consistent latent position estimation and vertex classification for random dot product graphs. *Pattern Analysis and Machine Intelligence, IEEE Transactions on*, 36(1):48–57, 2014.
- [44] M. Tang, A. Athreya, D. L. Sussman, V. Lyzinski, Y. Park, and C. E. Priebe. A semiparametric two-sample hypothesis testing problem for random graphs. *Journal of Computational and Graphical Statistics*, 26(2):344–354, 2017.
- [45] M. Tang, A. Athreya, D. L. Sussman, V. Lyzinski, and C. E. Priebe. A nonparametric two-sample hypothesis testing problem for random dot product graphs. *Bernoulli*, 23(3):1599–1630, 2017.
- [46] J. T. Vogelstein, W. G. Roncal, R. J. Vogelstein, and C. E. Priebe. Graph classification using signal-subgraphs: Applications in statistical connectomics. *Pattern Analysis and Machine Intelligence, IEEE Transactions on*, 35(7):1539–1551, 2013.
- [47] J. Yan, X. Yin, W. Lin, C. Deng, H. Zha, and X. Yang. A short survey of recent advances in graph matching. In *Proceedings of the 2016 ACM on International Conference on Multimedia Retrieval*, pages 167–174. ACM, 2016.
- [48] J. Yoder, L. Chen, H. Pao, E. Bridgeford, K. Levin, D. E. Fishkind, C. E. Priebe, and V. Lyzinski. Vertex nomination: The canonical sampling and the extended spectral nomination schemes. *arXiv preprint arXiv:1802.04960*, 2018.
- [49] M. Zhu and A. Ghodsi. Automatic dimensionality selection from the scree plot via the use of profile likelihood. *Computational Statistics & Data Analysis*, 51(2):918–930, 2006.
- [50] D. Zügner, A. Akbarnejad, and S. Günnemann. Adversarial Attacks on Neural Networks for Graph Data. *ArXiv e-prints*, May 2018.